Research Square

Preprints are preliminary reports that have not undergone peer review.
They should not be considered conclusive, used to inform clinical practice,
or referenced by the media as validated information.

Schrödinger's Cat spins your foods into digestion but only localized inside superfluids: A retrieval of rotational zeroing spin inertia Convergence Spectrum from Newton's Law of Universal Gravitation

Yi Yu Lai

yylai@innoen.org

Tsinghua University

Research Article

Keywords: translational zeroing, rotational zeroing, stochastic rotation, irrotational entropy, two-fluid data, spin inertia, convergence spectrum, linearity shifting collapse, Bohr spooky collapse

Posted Date: September 14th, 2026

DOI: https://doi.org/10.21203/rs.3.rs-11001912/v1

License: This work is licensed under a Creative Commons Attribution 4.0 International License.
Read Full License

Additional Declarations: No competing interests reported.

Schrödinger's Cat spins your foods into digestion but only localized inside superfluids: A retrieval of rotational zeroing spin inertia **Convergence Spectrum** from Newton's Law of Universal Gravitation

Yi Yu Lai (賴昱宇)[a,b]

[a]*Tsinghua University, Medical Science Building B343, Beijing, China*

[b]*Innoen®* *email: yylai@innoen.org*

7-315 Traders Blvd E, Mississauga, L4Z 3E4, Ontario, Canada

576 Pleasant View Driver #7, Lancaster, New York 14086, USA

Abstract

Newton's Law of Universal Gravitation stands as a cornerstone of modern science, asserting the universality of gravity by **translational zeroing**. General Relativity departed from the absolute and instantaneous action by introducing space-time curvature, yet it ultimately preserved the global-measurability of gravity. Quantum mechanics theoretically severed the connection between quantum states and gravity, leading the scientific community to accept the positive-manifold-originated-energy-based "Bohr spooky collapse" postulate, just unable to refute it. At its core, the Bohr–Einstein debate concerns whether the quantum state is fundamentally **universal** or **local**. Gravity is universally measurable, whereas quantum states are inherently uncertain and decoupled from gravity. If both are universal, why has quantum gravity which intends to reconcile them, become so insurmountable? Schrödinger was the first to recognize this tension; his famous "cat" was indeed designed to embarrass the quantum globalism. Landau should be the second to address this inconsistency, for his "two-fluid non-energy-consuming quantum state" is localized inside a superfluid rather than being universal.

We retrieve the non-simultaneous-rotational-zeroing entanglements embedded in Newton's universal law of gravitation, which were historically shielded by the translational-zeroing-rigid-time-Newtonian-Axiom. In our framework, quanta are neither confined to the microscopic world nor universal; they need a certain surface tension. For bio-systems, they are amplified by 10^9-level of $|\ G'_{rotational}\rangle$ validated by Cavendish mutation/*FHD* experiments. Such non-simultaneous-rotational-zeroing-stablized-structural amplifications are not only beyond the descriptions of Newton/Einstein but are also evaded by quantum mechanics as "a gravity-marginalized-quantum-state that will **irreversibly** collapse into a Newtonian eigenstate once measured". We take *EP*-inseparable-rotational-zeroing-entropy-based "**linearity shifting collapse**" to supersede historical-translational-zeroing-energy-based "Bohr spooky collapse", thereby retrieving the lost "quantum-gravity-non-simultaneous-**asymmetric-entropy-superposition** measurements" that had been eluded by the "spooky" drifting from intrinsically-symmetric-geometry.

Applying these localized **Gravitational/Planck-constant-shifting** quanta($\frac{|G'_{rotational}\rangle}{\hbar'_{Planck}} = \frac{1}{x^2}$) into bio-systems converges "weighted Le Châtelier's spin-inertia" that inverts *EP* for evolution. Drawing serendipity from long-standing-patterns of ancient Chinese dietary/herbal practices; we experimentally consolidate EB(**entropy-stabilized-barycenter**) steering biomembrane-selective-permeability. These EBs arise from dynamic "Entropy-ReverseFlow-*EP*-rotational-zeroing-spin-inertia-**convergence-spectrum**" rather than Newtonian "none-*EP*-translational-zeroing-rigid-mass-inertia", thereby suggesting a rotational zeroing revision of biology.

Keywords: translational zeroing, rotational zeroing, stochastic rotation, irrotational entropy, two-fluid data, spin inertia, convergence spectrum, linearity shifting collapse, Bohr spooky collapse

1. Introduction from History

1.1 Symmetric Sizeless-Point Geometry versus Asymmetric Reciprocal-Point Geometry

From Euclidean geometry to the later Riemannian and hyperbolic geometries, all are fallen into **sizeless point** geometres; which means starting from sizeless points, the arc length between points can be measured or calculated. This means geometries based on a pre-assumed symmetry. To understand the geometric origin of this innate symmetry, we can review the **Law of Entropy Degeneration** [1]:

$$\boldsymbol{n_k = n_{k+1} + |EP\rangle}$$

When this law was published, it only refers quantized entropy levels in superfluids, but its primitive form involves **asymmetric geometry**. Given $\boldsymbol{n_k}$ and $\boldsymbol{n_{k+1}}$ represent points at different positions along

an arc, because all points have neither size nor scale in traditional geometries, only a specific arc length between $\boldsymbol{n_k}$ and $\boldsymbol{n_{k+1}}$can be calculated; there is no position at which an $\boldsymbol{|EP\rangle}$ term can be introduced for them. Although a Riemannian manifold possesses flow characteristics, it still provides no position for $\boldsymbol{|EP\rangle}$. Its flow originates from parametric variation without the participation of $\boldsymbol{|EP\rangle}$ (we may call such a manifold the **positive-flow symmetric manifold** defined on **sizeless points**, whereas the manifold introduced for bio-systems may be termed a **Le Châtelier asymmetric entropyflow structure** based on **reciprocal points**: $\boldsymbol{n_k = n_{k+1} + |EP\rangle}$, here, the asymmetric "**reciprocal**" motion constitutes the basis of life).

Any form of geometry or algebra must undergo zeroing before application. The basis of symmetric geometry is an artificial pre-assumption of **absolute zeroability**. This can be understood by the Newton–Leibniz formula, which forms the basis of the **Newton Axiom** [1]:

$$f'(x) = \lim_{\Delta x \to 0} \frac{f(x+\Delta x)-f(x)}{\Delta x}$$

Here, $\Delta x \to 0$ constitutes zeroing. Regardless of the function involved, calculation is achieved through this limiting process, and only through zeroing can the calculation be completed. In a surface-tension region, Δx is regarded as EP, then $f(x+\Delta x)$ and $f(x)$ represent different points. It is therefore easy to understand why such a geometric system has difficulty accommodating EP: all transformations involved in its formulas proceed in the direction in which EP approaches zero (the discrete function or EP from a surface tension region is therefore presupposed to be **zeroed**).

From here, the fundamental distinction between symmetric sizeless-point geometry and asymmetric reciprocal-point geometry lies in whether $|EP\rangle$ is involved—or, more precisely, in the distinction between **translational zeroing** and **rotational zeroing**. In fact, translational zeroing, which contributed fundamentally to Newtonian mechanics, leaves little position for EP. By contrast, EP is intrinsic to rotational zeroing itself ($|EP\rangle$ can be understood simply as originating from a **non-rigid body**. It represents a parameter outside the domain defined by the Newton Axiom [1]. Traditional Euclidean geometry and the later non-Euclidean geometries, because of their intrinsic symmetry, methodologically contain no corresponding position for EP. Such geometries are generally suited to classical rigid body mechanics and energy conservation systems).

Historians have compared ancient Chinese geometry with Euclidean geometry and noted that Chinese records of the Pythagorean relation appeared earlier. The statement *"gou three, gu four, xian five"* (勾三股四弦五) recorded in the *Zhoubi Suanjing* and traditionally dated to the eleventh century BCE, together with Zhao Shuang's *Gougu Yuanfang Tu Zhu* (勾股圓方圖注, 222 CE), has been discussed in relation to Euclid's *Elements* (ca. 300 BCE) [2]. However, these historians may not have recognized that the Chinese method of deriving the gougu relation was, in its essential operation, a form of **asymmetric geometry**. It represents a geometric system outside Euclidean symmetric geometry. Because this system did not develop the axiomatic framework and symmetric geometry characteristic of Euclid, it was able to accommodate *EP*. Other technologies that developed alongside geometry in China during that historical period were predominantly asymmetric.

The divergent developmental pathways of symmetry and asymmetry in Chinese and Western geometry—and perhaps more broadly in technology—may have been influenced by the development of writtern language. For individuals raised with phonetic writing, symmetry may appear simpler, while asymmetry appears more complex. Conversely, for those whose native written language is logographic, asymmetry may appear comparatively natural, whereas constructing strict symmetry may require greater abstraction.

1.2 Define rotational/irrotational entropy from rotational zeroability

Classical definitions of entropy include the following:

Clausius entropy [3]: $$dS = \frac{\delta Q_{rev}}{T}$$

It describes the degree of disorder of a system or the "degradation" of energy, measuring the portion of energy unavailable for useful work. It theoretically assumes that a reversible process has the highest work efficiency (Note: the **reversible process** defined here is a **rigid reversible process without *EP***, which is fundamentally different from the ***EP*-sustained non-simultaneous reversible process** inside a superfluid discussed later).

Boltzmann entropy [4]:

$S = kBln\Omega$, where Ω represents the number of microscopic states of the system.

Shannon entropy [5]: $H = -\sum p_i log p_i$ (where p_i is the probability of occurrence of an event.)

Shannon entropy measures the amount of information required to eliminate uncertainty in a system, or equivalently, the average information content of an information source.

In addition to these representative entropy definitions, numerous extended forms of entropy have been developed. However, we should recognize that regardless of its particular formulation, **entropy is fundamentally the orthogonal error arising from non-zeroable rotation**. From Euclidean geometry and Galilean relativity to Newtonian physics, the Cartesian coordinate system has consistently employed a typical form of **translational zeroing** reference. To compare the running speeds of two individuals, they must first be placed on the same starting line; this is a simple example of the translational-zeroing method of comparison (note, their standing points must not involve rotation, or any difference in the rotational states of their starting points must be negligible. Without this condition, the zeroing method ceases to be valid). And this zeroing method has deeply embedded in the **Newton Axiom** [1].

To Einstein's work, although space was generalized into curved spacetime, the fundamental zeroing procedure remained translational in character. When rotating reference frames were involved, rotational problems were still transformed into a compatible translational zeroing. Einstein pursued throughout his life a unified theory capable of eliminating **observer effects** and establishing a more "equitable" reference framework. He increasingly recognized that the general covariance primarily establishes equivalence in the **form of physical equations**, whereas rotating and inertial reference frames can still exhibit fundamentally different physical effects. Rotational phenomena such as inertial frame dragging (such as Lense–Thirring effect), do not disappear merely because the equations are generally covariant.

The later **Einstein–Cartan theory** [6] introduced torsion, extending spacetime geometry beyond conventional symmetric Riemannian geometry into Riemann–Cartan geometry, in which the affine connection may contain an antisymmetric component and torsion can couple to the intrinsic angular momentum or spin. The introduction of torsion therefore gave spacetime geometry an explicit capacity to accommodate rotational degrees of freedom and represented **an important step** toward addressing **observer effects associated with rotational zeroing**. Nevertheless, this direction did not, during Einstein's lifetime, achieve his goal of a unified field theory capable of treating translational and rotational states within a single geometric framework while completely eliminating observer effects.

The subsequently developed **Gauge Field Theory** [7] further advanced the mathematical structures of connection and curvature, particularly through the complete formalism of local gauge fields in non-Abelian gauge theories. However, *non-Abelian* here refers to the noncommutativity of the gauge group and does not constitute genuine **rotational zeroing** itself. In other words, although gauge field theory substantially developed the mathematics of connections and curvature, its fundamental organizing principle remained **local gauge symmetry**, rather than continuing directly along the problem of rotational zeroing considered here. In particular, gauge field theory did not identify the ***EP* term** as characteristic of rotational zeroing. These limitations make gauge theory, despite its enormous success in high-energy physics, still more difficult to extend directly to bio-systems. These historical developments at least remind us of one point: **rotation is far more ubiquitous in nature than idealized translation**. Newton established classical mechanics through translational zeroing, greatly improving the reproducibility of experimental results and the stability of knowledge transmission. Nevertheless, translational zeroing remains a particular approximation to natural phenomena rather than a solution to the more general rotational zeroing problem.

The concept of entropy originated in thermodynamics. However, neither Clausius nor later investigators such as Boltzmann and Shannon recognized entropy is fundamentally a **rotational-zeroing problem**. Noether's theorem [8] established the relationship between symmetry and conservation laws. However, it did not address that symmetry itself originates from classical geometry, and that an energy-conservation framework is therefore secondary to geometric symmetry rather than

primary to it. Traditional symmetric geometry, as discussed before, intrinsically excludes *EP*. Entropy may certainly be described in terms of disorder, but **disorder** itself is not proposed here as the fundamental origin of entropy. The apparent disorder emerges when entropy that is intrinsically associated with rotational zeroing is **processed** within a **translational-zeroing reference frame**. The resulting disorder is therefore an inevitable consequence of the mismatch between two different modes of zeroing; a limitation originating partly from the zeroing structure of the mathematical tools themselves. The second law of thermodynamics is conventionally expressed in terms of entropy generation. However, this conclusion is also formulated using mathematical tools fundamentally organized around translational zeroing. If rotational zeroing is properly introduced, this directional interpretation may **need reversal under certain conditions**.

Once the rotational zeroing nature of entropy is recognized, a more general definition can be written: all forms of entropy represent **stochastic rotation**, or non-zeroable rotation beyond the zeroable rotation defined within a translational-zeroing reference frame. In nature, any interaction that cannot be zeroed can manifest as irregular **stochastic rotation**, or more precisely as rotational behavior that cannot be transformed into translational zeroing. This can be illustrated using a Newtonian expression:

$$F = m\omega^2 r$$

A basic condition underlying this centripetal-force description is that the rotating mass of a rigid body can be referenced to a rotational center that converges to a geometric point, thereby permitting a zeroing condition, or the rigid body itself excludes EP. A water vortex is fundamentally different. Its rotating components do not necessarily share a single fixed rotational center; the rotational center may fluctuate over a finite region rather than converge to a geometric point, with *EP* **necessarily** involved. Such a system therefore exhibits **non-zeroable rotation** and cannot be represented by conventional Newtonian/Einsteinian or existing physical descriptions based primarily on translational zeroing.

Moreover, even when only considering the translational-zeroing reference frame inherited from Newtonian mechanics, rotation can arise extremely easily even for **rigid bodies**. Consider the collision of two small balls. Only when their centers of mass are aligned along the same line can the interaction be treated as an ideal translational-zeroing problem. A slight displacement away from this center-of-mass line inevitably generates rotational components, many of which may develop into uncontrolled stochastic rotation. Such stochastic rotations fall outside the descriptive capability of a translational-zeroing reference frame, while an appropriate rotational-zeroing tool remains absent. This constitutes the origin of chaotic entropy in physics. Simply speaking, *chaotic* here refers to behavior that necessarily appears chaotic relative to a translational reference frame. It does not imply that nature **has** an inherently chaotic tendency in the absence of an artificially imposed translational-zeroing reference frame. In this sense, the conventional concept of chaos already contains an implicit Newton-Axiom [1] presupposition that translational zeroing provides the fundamental reference for physical laws.

Rotational Entropy and Irrotational Entropy

From here, the previously discussed entropies—including Clausius entropy and Boltzmann entropy, etc.—can be regarded as particular manifestations of the more general category of **stochastic entropy**. Once this rotational basis of entropy is introduced, **irrotational entropy** can also be defined:

Irrotational entropy refers to an internal low-relative-rotation entropy-level state produced under specific *EP*-sustaining conditions (stable irrotational entropy in bio-systems is achieved through bidirectional inversion flow along the spinal vector. The presence of *EP* means that adjacent irrotational entropy levels may approach one another in rotational velocity but can never attain absolutely identical rotational velocities, that is, in $\boldsymbol{n_k = n_{k+1} + |EP\rangle}$, $\boldsymbol{n_k \neq n_{k+1}}$, and the difference between $\boldsymbol{n_k}$ and $\boldsymbol{n_{k+1}}$ cannot be represented by traditional parameters due to Le Châtelier's effects**).** The concept of **irrotational entropy** was initially developed from an extension of Landau's two-fluid model [1]. That model described a state capable of motion without conventional dissipation of system energy. Although Landau did not identify the existence of *EP*, his model can nevertheless be regarded as one of the closest established physical descriptions of ***EP*-zeroable rotation** (two rotational-zeroing methods can be distinguished: Newtonian rigid-body rotation converted into translational zeroing, in which rotational centers are theoretically assumed to converge to a single geometric point without *EP*; and biological spinal-vector rotational zeroing, in which rotational centers undergo inversion inside a superfluid structure to steer peripheral structures and require *EP* for sustaining. We therefore refer to the latter as *EP*-zeroable rotation, and to the former as non-*EP*, symmetric-geometry-zeroable rotation).

We should also recognize that converting ubiquitous rotational entropy into irrotational entropy is not so difficult to observe experimentally. The wall-climbing behavior of a low-temperature superfluid

provides a typical example of an **irrotational-entropy state**, and such a phenomenon can be reproduced within an ordinary laboratory timescale. What is substantially more difficult is the direct observation of **non-living rotational entropy transforming into a living, stabilized bi-directional irrotational-entropy structure**. The emergence of the earliest life on Earth has been estimated to have required approximately **0.2–0.8 billion years** [9]. To observe experimentally the transformation from non-living rotational entropy into even the simplest living irrotational entropy structure would therefore, require simulation of the physical processes associated with the earliest stages of natural biological evolution over such geological timescales. To date, no laboratory in the world has yet reproduced the complete evolutionary physical process of the origin of life on this scale.

1.3 Non-Simultaneous "Two-Fluid Data Structure" Combining Rigid Translational Zeroing and Surface Rotational Zeroing

The Newton–Leibniz formula is a typical rigid-body zeroing operation. Whether for rigid or non-rigid bodies, zeroing remains essential—but in the latter case, the zeroing oscillates within a finite range rather than converging to the geometric zero presupposed in standard calculus. A parameter can expressed as:

$$(\boldsymbol{x} + |\boldsymbol{x}'\rangle, \boldsymbol{y} + |\boldsymbol{y}'\rangle)$$

Traditional rigid-body mechanics assumes that the point can be absolutely zeroed, the above point is therefore reduce to $(\boldsymbol{x}, \boldsymbol{y})$. In the real world, only an absolutely ideal rigid body can make the non-rigid-body term $(|\boldsymbol{x}'\rangle, |\boldsymbol{y}'\rangle)$ equal to 0; in the overwhelming majority of parameter changes, it is not 0. We can therefore simply call this term the surface-tension region, while $(\boldsymbol{x}, \boldsymbol{y})$ is called the Newtonian rigid-body term. From the perspective of the rigid-body region and the surface-tension region, as long as the surface-tension region is not 0, zeroing in this region takes the following form:

$$f'(x) = \lim_{|\boldsymbol{x}\prime\rangle \to EP} \frac{f(x+|\boldsymbol{x}\prime\rangle) - f(x)}{|\boldsymbol{x}\prime\rangle}$$

(Note that Riemann smoothness can no longer be satisfied here. In addition, although *EP* can be regarded as the minimum discrete unit of a surface-tension system, it is not a fixed Planck length; the fluctuation range of *EP* under surface tension is wide. In addition, $\frac{\mathrm{d}}{\mathrm{dx}}\boldsymbol{cos\ (nx)} = -(\boldsymbol{n}\,\boldsymbol{x})$, $\frac{\mathrm{d}}{\mathrm{dx}}\boldsymbol{sin(nx)} = \mathbf{cos}\ (\boldsymbol{n}\,\boldsymbol{x})$ may avoid the requirement of tending to 0). In traditional translational-zeroing geometry, after zeroing a quantity can in theory be measured precisely. Here, it is zeroed to a non-zero *EP* having a certain length. Because the two ends of this length are asymmetric, they cannot be measured simultaneously. This is a non-simultaneously measurable quantity. This result is consistent with the statement of Heisenberg's uncertainty principle, though the zeroing method involved differs. Classical quantum mechanics uses commutation to express non-simultaneous measurability, but in fact both eigenstates and uncertainty quantum states use translational zeroing. In our two-fluid data structure, the "+" sign links one translational zeroing and one rotational zeroing. The uncertainty quantities produced by two different zeroing methods are closer to the actual situation. And this method is extremely convenient both theoretically and in practical biological applications.

From here we can define non-simultaneous time (or intrinsic aging time): in traditional symmetric geometry, what occurs between two rigid and zeroed points is rigid time, for example between $(\boldsymbol{x_1}, \boldsymbol{y_1})$ and $(\boldsymbol{x_2}, \boldsymbol{y_2})$. Whereas what connects two non-zeroed points, for example between $(\boldsymbol{x_1} + |\boldsymbol{x_1}'\rangle, \boldsymbol{y_1} + |\boldsymbol{y_1}'\rangle)$ and $(\boldsymbol{x_2} + |\boldsymbol{x_2}'\rangle, \boldsymbol{y_2} + |\boldsymbol{y_2}'\rangle)$, is non-simultaneous time. (Note that non-simultaneous time must be maintained by *EP*. This is also why life is finite. Once both points are zeroed into a relatively static state and lose enough dynamic *EP*, it means death for a bio-system. More precisely, death represents the loss of unsymmetric-entropy availability or the CvS we'll discuss later and retrogression toward a state in which only symmetric Noether energy is available.) Non-simultaneous time is actually more universal than rigid time that is an approximation under certain conditions. For any given two-fluid parameters, neither term can be 0. The assumption of early Newtonian rigid-body mechanics that one

term was 0 merely reflected the level of technical detection at that time, and does not mean that it is truly 0. Bio-systems are structured in the opposite direction from Newtonian rigid-body mechanics: almost all is in $(|\boldsymbol{x}'\rangle, |\boldsymbol{y}'\rangle)$ term while the $(\boldsymbol{x}, \boldsymbol{y})$ term is very small, but even in this case this $(\boldsymbol{x}, \boldsymbol{y})$ term is still not 0. (Note: gravity is written as $\boldsymbol{F} + |\boldsymbol{F}'\rangle$, in traditional theory the term $\boldsymbol{F}$ is the rigid symmetric translational-zeroing term, whereas the new term $|\boldsymbol{F}'\rangle$ is the asymmetric rotational-zeroing term of the surface-tension region. Classical quantum mechanics in fact incorrectly applies translational zeroing where rotational zeroing should dominate. To resolve the resulting inconsistency, the Copenhagen school marginalized gravity, claiming that gravity can be neglected in the Schrödinger equation, while avoiding the fact that such neglect is only conditional and will increase geometrically with asymmetric-bio-quantum-superposition. The superposition used in traditional quantum mechanics is actually symmetric superposition, perhaps another reason why gravity had to be marginalized. With respect to symmetry, classical quantum mechanics is even more faithful to the Newton Axiom [1] than relativity. Einstein–Cartan theory still attempted rotational zeroing, whereas quantum mechanics directly compressed spin into pseudo-rotational zeroing, in effect returning to the translational-zeroing system of the early Newtonian era.) de Broglie proposed matter waves $\boldsymbol{\lambda} = \frac{\boldsymbol{h}}{\boldsymbol{p}}$, but it was not recognized that the momentum here can only come from $(|\boldsymbol{x}'\rangle, |\boldsymbol{y}'\rangle)$ and not Newtonian momentum in the corresponding term $(\boldsymbol{x}, \boldsymbol{y})$, because Newtonian momentum $\boldsymbol{mv}$ is theoretically symmetric translational-zeroing momentum excludes *EP*, whereas momentum in the term $(|\boldsymbol{x}'\rangle, |\boldsymbol{y}'\rangle)$ is asymmetric rotational-zeroing superposition momentum and must be sustained by *EP*.

1.4 The essence of the Bohr–Einstein debate: quantum localization.

Einstein's theory originated from the globally measurable gravity of the Newtonian era, and the measurability he referred to in the Bohr–Einstein debate in fact also presupposed quantum globality: he hoped to use the globality of gravity to measure quantum globality. Bohr himself advocated quantum globality but could not give a reasonable explanation for it, and the debate later even developed toward psychological wording ("the moon does not exist when it is not thought about"). His incompleteness lay precisely in not recognizing that the quantum is localized even in the microscopic world. Bohr Spooky was not his fault, but the fault of the traditional symmetric geometry. To adapt to the symetric geometry, the defects produced by the globalizing misdirection of classical quantum mechanics include the following: ① continuously adding quantum numbers—principal quantum number (n), angular quantum number (l), magnetic quantum number (m_l), spin magnetic quantum number (m_s), etc.—using additional quantum numbers to replace and exclude *EP*, or in other words requiring no *EP* among quantum-number levels; ② operatorization and the definition of Hilbert space: the mathematical tool of Hilbert space itself presupposes quantum globality, or classical quantum mechanics in its definition of Hilbert space did not recognize that the quantum is intrinsically localized; ③ the introduction of spin $(\boldsymbol{L} = \boldsymbol{r} \times \boldsymbol{p})$ proves that even classical quantum mechanics cannot escape rotational zeroing, but it is nevertheless treated through angular-momentum conservation and similar approaches as translational zeroing (that is, a problem requiring *EP*-rotational-zeroing is renamed an "intrinsic property" to elude the *EP*). This pseudo-rotational zeroing can only be regarded as an approximate treatment of classical quantum mechanics and completely departs from the intrinsic nature of quantum rotational zeroing; ④ the fundamental defect produced by the preceding defect is the marginalization of gravity. This is precisely the jinx of quantum gravity. From classical quantum mechanics onward, many later efforts, such as M-theory and loop quantum theory, have faced insurmountable difficulties. These difficulties are all barriers produced by the original globalization of the quantum. We should emphasize that even in the microscopic world, the quantum must be localized; without a quantum-localization model, quantum gravity cannot achieve any substantive breakthrough. (Later LQG, although introducing spin networks, still follows the original path of globality and cannot form a spinal vector through an *EP* surface-tension region; one may say that a spin network differs from a surface-tension region only by *EP*. Here, we need to emphasize the distinction between the state vector of classical quantum

mechanics and the spinal vector operating in bio-systems: whereas the former is constructed on symmetric geometry using sizeless points, the latter is composed of asymmetric reciprocal entropy points: $\boldsymbol{n_k = n_{k+1} + |EP\rangle}$.) Regarding quantum localization, we can even derive it directly from the two-fluid parameter structure: $(\boldsymbol{x} + |\boldsymbol{x}'\rangle, \boldsymbol{y} + |\boldsymbol{y}'\rangle)$, whether applied in the microscopic or macroscopic world, as long as the term $(\boldsymbol{x}, \boldsymbol{y})$ is not 0, the quantum must be localized. Using the extremely low-probability model of a globally quantized state to handle quantum gravity is a dead end. (Interestingly, quantum gravity, made extraordinarily difficult for physicists by the bias of quantum globality, is quite simple in biology. Among life forms on Earth, regardless of species, evolutionary level, or whether extant or extinct, one cannot even find an exception that violates quantum gravity. Life can be said to be an inevitable result and a real terrestrial reappearance of quantum gravity.)

The work in **Sections 1.1–1.3** of this paper was involved in previous articles, but the content beginning with **Section 1.4**—such as quantum localization, translational/rotational zeroing, the Le Châtelier's-effect term of gravity, and spin inertia (an upgrade of the previous bio-inertia concept) — appears for the first time in this paper, and similar material has not been reported in any literature by others. For the Le Châtelier's effect, the forces involved in Newton's three laws and the force involved in gravity differ in the structural strength of their two-fluid parameters. If gravity is written as $+|\boldsymbol{F}'\rangle$, then this structural strength far exceeds the two-fluid structural strength of other forces involved in Newton's three laws. (Historically, the basis of Einstein's relativity, gravitational mass = inertial mass, holds only when $|\boldsymbol{F}'\rangle$ can be completely neglected. Once $|\boldsymbol{F}'\rangle$ increases even slightly, this basis of general relativity can no longer exist. In addition, Einstein's geometric gravitational effect in general relativity involves only the $(\boldsymbol{x}, \boldsymbol{y})$ term; its calculated value is far below the value obtained under the asymmetric superposition of $(|\boldsymbol{x}'\rangle, |\boldsymbol{y}'\rangle)$, and it still does not escape the rigid system.) Note that although the relevant term $|\boldsymbol{F}'\rangle$ in the law of universal gravitation is extremely weak for a Newtonian rigid body and is confined to the surface-tension region, this weak rotational-zeroing term does follow the Le Châtelier principle. If dust or various debris has fallen on a soap bubble, when the next dust particle falls on it, the dust and debris that previously fell on the bubble will move in a direction that reduces the effect of the newly falling particle. This is the surface Le Châtelier effect. Note that this is an entropy-preservation driving force rather than a traditional energy-conservation driving force. Moreover, even on the hardest solid we see, the surface still undergoes Le Châtelier motion in the same way as the surface of a soap-bubble film; only the intensity differs. No matter how hard the solid is, it cannot make the relevant term $|\boldsymbol{F}'\rangle$ become 0. Different objects that we observe merely differ in the proportions of the rigid-body term $\boldsymbol{F}$ and the Le Châtelier term $|\boldsymbol{F}'\rangle$; the rigid-body term $\boldsymbol{F}$ employs translational zeroing, whereas the Le Châtelier term $|\boldsymbol{F}'\rangle$ takes rotational zeroing. This may be why traditional physics had to omit the surface-tension region.

From here, it is easily understood that the strength of non-living material is completely different from that of living matter. Non-living matter follows a positive-flow symmetric manifold, meaning that the material strength or the direction of energy flow aligns with the manifold direction, so it can be approximately treated as having strength proportional to the amount of forward flow. In contrast, the Le Châtelier's flow asymmetric manifold in living matter means that material strength is closely tied to the reverse inversion entropyflow. For example, the material strength or force between two muscles cannot be calculated from the forward flow between them; instead, it must be determined by the reverse Le Châtelier's inversion entropyflow intensity between the two muscles. Superficially, this entropyflow appears opposite in direction to the routine energy flow. All these flow directions are simply originated from our two-fluid data structure: $(\boldsymbol{x} + |\boldsymbol{x}'\rangle, \boldsymbol{y} + |\boldsymbol{y}'\rangle)$

Strictly speaking, even wave particle duality in traditional quantum mechanics is essentially a two-fluid data format. Wave particle duality originated in de Broglie's 1924 doctoral thesis on matter waves; Bohr later proposed the complementarity principle in 1927 and held that the two cannot exist simultaneously. This is also a deviation caused by symmetric superposition. If quantum superposition is restored to an asymmetric linearity shifting superposition, wave and particle properties will coexist, neither term will be 0, and only their proportions will differ. This coexistence is closer to our entropy

preservation model, but it directly denies Bohr spooky collapse. As long as even extremely weak translational zeroing and rotational zeroing coexist, collapse requires time and cannot reach spooky speed. Historically, Bell-inequality experiments could only demonstrate the existence of quantum states, but were mistakenly used to prove the spooky speed of quantum entanglement, allowing the Bohr Spooky Collapse postulate to prevail for nearly a century. Bell inequalities in fact cannot verify the speed of entanglement; they can only verify that quantum states indeed exist.

1.5 Symmetric and asymmetric modes of quantum superposition

1.51 **Bohr Spooky Collapse** vs. **linearity-shifting collapse**

For the **linearity-shifting model**, it can be obtained from $\boldsymbol{n_k = n_{k+1} + |EP\rangle}$. Suppose that the $\boldsymbol{n_k}$ and $\boldsymbol{n_{k+1}}$ have $\boldsymbol{m}$ and $\boldsymbol{n}$ levels respectively, $\boldsymbol{m \neq n}$. During dynamic superposition, necessarily only part of $\boldsymbol{m}$ or $\boldsymbol{n}$ can be superposed. The superposed part forms the superfluid, while the non-superposed portions of $\boldsymbol{m}$ and $\boldsymbol{n}$ constitute the normal-fluid component (also called the peripheral structure in a bio-system). Neither the superfluid nor the normal-fluid can exist independently. Consequently, asymmetric superposition appears as continuous linear back-and-forth shifting, and the resulting structure is called a linearity-shifting structure. (Here shifting is actually the key to *EP* intake. The traditional quantum-mechanical postulate of symmetric state superposition does not involve linearity shifting/*EP*. The deeper origin of Bohr Spooky Collapse is precisely the absence of *EP*). Now, we can summarize the difference between classical Bohr Spooky Collapse and our Linearity Shifting Collapse as follows:

The measurement-collapse mechanism of classical symetric quantum mechanics, Bohr Spooky Collapse, inevitably treats the external world as an appendage of instrumental detection rather than as a physical constraint that the quantum state itself must satisfy. Superposition in this framework is a symmetric operation in Hilbert space: $|\psi\rangle = \sum \boldsymbol{c_i}\,|\,\boldsymbol{i}\rangle$, and collapse is essentially an **irreversible** fall toward a Newtonian eigenstate. It follows the energy-conservation paradigm—the Hamiltonian, as a global generator, governs the unitary evolution of the entire closed system, with energy distributed among all degrees of freedom. Behind this lies a series of interconnected theoretical defects: separating the quantum state from the environment (failing to recognize the decisive role of *EP*), the opposition between symmetric and asymmetric superposition, rigid global time vs. non-simultaneous time, degradation of rotational zeroing into translational zeroing, and rigid presuppositions concerning gravity and the Planck scale.

Global energy conservation vs. local entropy preservation. Standard quantum mechanics follows the energy global conservation law. Linearity-shifting collapse is local, and its core principle is entropy preservation: evolution of a quantum state in a local reference system does not pursue energy minimization, but maintains the dynamics of local entropyflow. The physical carrier of this paradigm is surface tension—the quantum state cannot exist independently of the interface that carries it. Surface tension provides the geometric boundary of local constraint, allowing quantum coherence to **continue oscillating** in an open dissipative system rather than undergoing a one-time irreversible collapse. Inside the **superfluid** state, this oscillation can proceed without dissipating the system's energy, thereby **permitting** reversible/reciprocal collapse (**linearity shifting collapse**). The duration of reversible/ reciprocal collapse simply defines non-simultaneous time. The conventional "**Bohr spooky collapse**" implicitly **excludes reversible/reciprocal collapse, yet provides no evidence** that such collapse cannot occur, even in its traditional described scenario where no surface tension region is involved (note: even under such conditions, partially reciprocal collapse remains unavoidable).

1.52 Rigid Time vs. Non-Simultaneous Time

The time *t* in the Schrödinger equation is a rigid global parameter; $i\hbar\frac{\partial}{\partial t}\psi=\hat{H}\psi$, means that the entire universe shares the same clock. Although the Dirac equation introduces relativistic covariance, its time coordinate still exists as a parameterizable background dimension and does not depart from the global-time paradigm (global time is related to quantum globality). The non-simultaneous time adopted here means that each local reference frame carries its own temporal generator. The evolution of this temporal generator is driven by the rotational-zeroing stability of local entropyflow rather than by the ticks of a global clock. In other words, the quantum state itself carries an intrinsic aging time related to the gravitational constant/Planck constant. This is the fundamental reason why living systems are finite and why individual aging curves differ, and it is also the reason why quantum states must be localized rather than globalized.

Rotational zeroing is degraded into translational zeroing. Conservation of angular momentum corresponds to spatial rotational symmetry, and quantum mechanics should in principle employ rotational zeroing—defining physical angular momentum by eliminating the rotational background in a local reference frame. However, although the standard treatment of spin can algebraically be regarded formally as rotational zeroing (a nontrivial representation of the SU(2) group), its operational essence is degraded into translational zeroing: spin lacks dependence on spatial coordinates and also lacks coupling to *EP*. This "de-spatialization" means that although spin ($\mathbf{L} = \mathbf{r} \times \mathbf{p}$) is called rotational, in practice it still remains within the translational-zeroing paradigm—that is, this rotational zeroing is actually only an approximate scheme degraded into translational zeroing. It is not difficult to understand that the reason spin has had to be treated by translational zeroing is still the obstructive effect of quantum globality. Without a quantum-localization model, no method can achieve genuine rotational zeroing.

Marginalization of gravity and the Planck scale. The Schrödinger equation assumes that gravity can be neglected at the atomic scale—$\hbar$ governs the microscopic domain, while G is relegated to macroscopic celestial bodies. Cavendish mutation/*FHD* experiments [10] reproducibly revealed that the difference in gravitational signals between living and dead biological bodies can reach a magnitude of 10^9. This means that G is not a universal constant, but a dynamical variable sensitive to the non-simultaneous time of the new quantum state. G can also be composed of two-fluid data and written as $\boldsymbol{G_{gravitational} = G_{Cavendish} + | G'_{rotational} \rangle}$. Such gravity amplification is produced when the corresponding term $|\boldsymbol{G'_{rotational}}\rangle$ in the two-fluid data of universal gravitation is highly folded in a biological body and coupled with environmental *EP*, resulting in an overall apparent measured value far above that described by Newtonian/Einsteinian formulas. In addition, accompanying this drift of G, $\hbar$ likewise undergoes a systematic shift—the quantum coherence length is no longer locked to the atomic scale (~10^{-10} m), but extends macroscopically with *EP* intensity. The biological spinal column (macroscopic scale ~10^0 m) therefore lies within the governing range of quantum coherence. The quantum–classical boundary is determined by the ratio of G to $\hbar$ in the local reference system rather than by rigid constants. In biological systems, the gravitational signal was experimentally measured as amplified by 10^9. Because this amplification of the gravitational constant involves only the biologically quantized component, a Dirac symbol is added.

For $|\boldsymbol{G'^{\ bio-system}_{rotational\ zeroing}}\rangle = \boldsymbol{G^{Newtoinian\ rigid\ body}_{translational\ zeroing}} \times 10^9$, if the Planck length is extended to the DNA scale, $\boldsymbol{L'_{Planck}}$=L (base spacing, 3.4 × 10^{-11} m; DNA pitch, 3.4 × 10^{-10} m), a new Planck constant $\boldsymbol{L'_{Planck}} = \sqrt{\boldsymbol{G'\hbar'/c^3}}$ can be derived, and $(\frac{|\boldsymbol{G'_{rotational}}\rangle}{\hbar'_{Planck}} = \frac{1}{x^2})$ can be further obtained. Note that the inverse-square result here is obtained by extending the Planck constant to the DNA range. Whether such an extension is reasonable remains to be further verified. However, this dynamic ratio method between the Newtonian rigid-body term and the surface-tension term has physical significance in biological structures driven by biological EB (entropy-stabilized barycenter) [11]. Differences in evolutionary degree among species, or differences in aging degree among individuals of the same species, can all be reflected in *EB*.

Linearity Shifting Collapse is opposite to the above defects. Its core quantum-superposition operation is not symmetric, or in other words involves symmetry breaking and transfer: in the formula $\boldsymbol{n_k = n_{k+1} + |EP\rangle}$, $\boldsymbol{n_k}$ collapses to $\boldsymbol{n_{k+1}}$, and $\boldsymbol{n_{k+1}}$ collapses back to $\boldsymbol{n_k}$. As long as *EP* is available, the system dynamically resides in this reversible/reciprocating collapse rather than **irreversibly** falling into a Newtonian eigenstate. This is fundamentally different from Bohr Spooky Collapse, in which "once the condition is reached" there is a one-time terminal **irreversible** fall into a Newtonian eigenstate. Linearity Shifting Collapse is a continuous, reversible oscillatory process and realizes non-perturbative amplification of gravitational effects. This is the mechanism revealed by the Cavendish mutation/*FHD* experiments [10]. It should be emphasized that this process intakes *EP* and must be maintained by EP. Classical quantum mechanics mistakenly assumes that *EP* is not involved, and this defect has seriously constrained the discipline from moving toward the entropy-preservation paradigm. Linearity shifting is local and rotationally zeroed, and requires surface tension or quantum-localization *EP* for maintenance.

Classical quantum mechanics, under the concept of quantum globality, uses non-commuting operators to represent non-simultaneous measurability. Under the premise of quantum-state localization, however, only by instead using translational zeroing/rotational zeroing to represent non-simultaneous measurability can the framework enter macroscopic bio-systems or *EB* regulation [12]. *EP* forms an *in vivo* environment through multilayer superposition, implying inversion between the maximum and minimum scales of the system. Bohr Spooky Collapse is an expedient measure under the traditiaonl geometric form that excludes *EP*; however, even for the conventional quantum mechanics of non-biological systems, it actually contains deviations, because non-global quantum states all require *EP*.

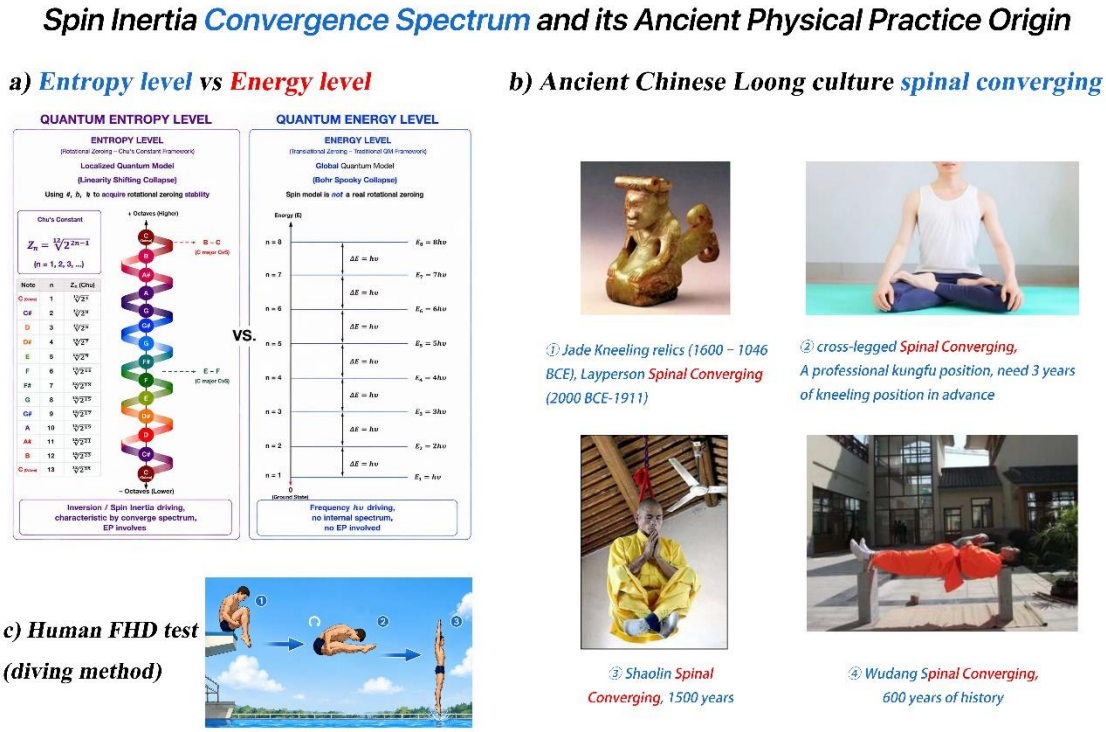
Timeline for the establishment of the Linearity Shifting Collapse framework: this model is based on Landau's two-fluid theory (published in 1941), and its theoretical structure was only completed at the end of 2025. Its key foundation, the Cavendish mutation experiments, was preliminarily completed during 2014–2016 in Medical Science Building B343 of Tsinghua University. The *FHD* experiments were first completed on February 15, 2020, at the Etobicoke Olympium in Ontario, Canada. Retrospective historical corroboration was also identified in ancient Chinese medical theory, with a history of more than 2,000 years, as well as in the traditional practices of Chinese Shaolin and Wudang Kungfu, with histories of approximately 1,500 and 600 years. Ancient Chinese practitioners already knew that the spine regulates different parts of the body through linearity shifting—in today's terminology, this means obtaining non-simultaneous time. Specifically, linearity shifting occurs between two non-zeroed points; in humans, this is the flow of CSF between the vertebrae, maintaining rotational-zeroing regulation of the whole body according to entropy preservation. In medicine, after a CSF tap, a person must lie still for three hours and must not move; otherwise, the body may suffer a severe aging-impact injury, because CSF tap affects the zeroing of different parts of the body and therefore requires rest for recovery. This modern clinical evidence corroborates the spinal-training system of ancient Chinese kung fu. (CSF tap was first introduced clinically by Quincke in 1891 [12]; since then, there has been the practical experience that a person must remain recumbent for three hours after a CSF tap.)

1.6 Rotational Zeroing Convergence Spectrum fingerprint originated from music harmonics

Rotational zeroing, which has been difficult for modern physics to solve from the Newtonian era through the most recent physical theories, actually had a solution for asymmetric rotational superposition in music long ago. The ancient Chinese scientist Chu Tsai-Yü first created twelve-tone equal temperament in 1581 [13], and his work was introduced to Europe in translation around 1779. Thereafter, twelve-tone equal temperament gradually became the common tuning standard for piano and modern music. The standard was established 445 years ago, and its large-scale successful industrial application dates back about 270 years. Here we call the relevant pitch quantity $\sqrt[12]{\boldsymbol{2^{2n-1}}}$ in musical harmonics as Chu's constant. **(Fig. 1a)** shows the difference between entropy levels and energy levels.

Figure 1. Spin Inertia Convergence Spectrum and its Ancient Physical Practice Origin

(a) Entropy Level vs Energy Level (b) Ancient Chinese Loong culture spinal converging (c) Diving Posture for Stabilizing *FHD* Measurements from a 10-Meter commercial Platform



Here, we provide the background for this figure, with the following Chu's constant C-major scale:

Scale: C: $\left|\sqrt[12]{2^{2-1}}\right\rangle$ D: $\left|\sqrt[12]{2^{4-1}}\right\rangle$ E: $\left|\sqrt[12]{2^{6-1}}\right\rangle$ **F**: $\left|\sqrt[12]{2^{8-2}}\right\rangle$ G: $\left|\sqrt[12]{2^{10-2}}\right\rangle$A: $\left|\sqrt[12]{2^{12-2}}\right\rangle$ B: $\left|\sqrt[12]{2^{14-2}}\right\rangle$, Ċ: $\left|\sqrt[12]{2^{(2-1)+12}}\right\rangle$

C root - triad: C: $\left|\sqrt[12]{2^{2-1}}\right\rangle$., E: $\left|\sqrt[12]{2^{6-1}}\right\rangle$, G:$\left|\sqrt[12]{2^{10-2}}\right\rangle$

in the C major scale C-D-E-F-G-A-B, there are only half-steps for E–F and B–C ($step\ of\ which\ in\ \sqrt[12]{\mathbf{2^{2n-1}}}$ is **1**) and those between others are full step (step of which in $\sqrt[12]{\mathbf{2^{2n-1}}}$ is 2). We can call them as **convergence spectrum**. A sheet music is constructed by **rotational zeroing** of a melody by its proper accompaniment, or notes combine with the inversion of their chords. The simplest muiscal chord is a triad (only three notes) and the largest is a thirteenth chord). Like a C note, root triad: C-E-G **(1, 5, 8)**, first inversion: E–G–C **(5,8,i̇),** and the second inversion G–C–E **(8,i̇,5̇)** , each triad's inversion means an octave shifting of root position. Following the equation of **n – 1**, a thirteenth chord has 13-1=12 inversions while a triad only has 2 inversions. It must be noted that chord use and chord inversion must keep the intervals (distances) between the different inversions unchanged. For example, in a C triad, the distance between the root to the first inversion is four semitones (C-C♯-D-D♯-E), and those between the first to the second inversion is three semitones (E-F-F♯-G). Therefore, regardless of where the triad is located or how it is inverted, this **distance structure** must be maintained (note carefully that **symmetric superposition** preserves equal distances among spins (here equivalent to inversions), whereas **asymmetric superposition** produces unequal inversion-level-to-inversion-level distances, thereby propagating the underlying asymmetry inside superfluid. **By the same asymmetric superposition mechanism**, the vertebral segments of the human spine are not uniform in size; this structural differentiation preserves asymmetric superposition across all levels of the somatic system, making the spine the largest pool of quantum-gravity asymmetric superposition in

the human body. Senility, accordingly, corresponds to the progressive loss of asymmetry in CSF flow of the somatic spinal system). Therefore, the sharp (♯), flat (♭), and natural (♮) symbols commonly used in music can be regarded as "rotational zeroing inversion **operators** (functioning similarly to quantum-mechanical operators, except that classical quantum-mechanical operators operate within **symmetric geometry**, whereas the musical operators considered here perform **genuinely asymmetric operations**) in accordance with this asymmetric superposition principle. Later we will see how the stability of these asymmetric-chord-inversion distances constitutes the stability of the **convergence spectrum** and can be defined the fingerprint of spin inertia (Convergence Spectrum is abbreviated as **CvS** hereafter in this paper to avoid confusion with other terminological abbreviations).

1.61 Basic differences between energy levels and entropy levels - convergence spectrum (a fingerprint originated from asymmetric inversion/spin inertia)

From **(Fig. 1a)**, we can see several major specific differences between the energy levels of traditional microscopic global quantum mechanics (pseudo-rotational zeroing, based on particle presence probability, randomly regulated) and entropy levels localized in a superfluid (real rotational zeroing, based on entropy preservation of the spinal vector/peripheral structure under a surface-tension region, regulated by Chu's constant inversion inertia):

In global quantum states, symmetric Noether energy levels differ by an energy unit, $E = nh\nu$ (independent of *EP*), whereas asymmetric Chu's constant entropy levels in localized superfluid quantum states differ by inversion inertia constituted by the relevant relation (requiring *EP* sustainment). In an energy level, frequency determines the energy level, $E = nh\nu$, one frequency $h\nu$ completely determines one energy level, and the relation is unique. An entropy level, however, cannot be determined by frequency/pitch alone. It requires **frequency plus inversion inertia**. For example, the note C may occur in the root position or occupy a particular inversion of a chord. As described in the background section, regardless of its position, the note must maintain the characteristic intervallic distance of a running inversion, which means this C note possibly in its root position, or D reduce a semitone, or B elevate a semitone,etc. These downward or upward pitch adjustments constitute the **operations** through which inversion inertia is maintained. In summary, pitch (frequency) together with the interval and inversion of its position is required to determine the function of the entropy level, and they must correspondingly entangle through the Le Châtelier effect. (The entanglement here is fundamentally different from traditional quantum entanglement; it is only Le Châtelier-effect entanglement, not Bohr spooky collapse entanglement in tradition.) At the root, inversion inertia here is precisely what disappeared when traditional quantum mechanics treated spin as pseudo-rotational zeroing, leaving only frequency. (The term pseudo-rotational zeroing is used because all rotational zeroing intakes *EP* to different degrees, whereas rotational zeroing treated by a translational approximation is theoretically regarded as not taking in *EP*; therefore, this type of rotational zeroing without *EP* intake can only be called pseudo-rotational zeroing.) An entropy level is real rotational zeroing, so inversion inertia plus frequency jointly determines the function of an entropy level. This musical inversion inertia can also be called spin inertia in physics.

Different inversions of the same pitch, or the dynamics of Le Châtelier rotational-zeroing inertia, express entropy-preservation regulation between the spinal vector and peripheral structure, and have little relation to the probability of appearance of the carrier in a quantum entropy level. Energy levels, however, are described in quantum mechanics in terms of the probability of particle appearance. This raises a key issue: ether is a concept abandoned by the scientific community, and energy levels naturally adapt to this abandonment, hence the description in terms of global stochastic probability; this probability description is also one factor producing Bohr Spooky Collapse. By contrast, entropy levels require concepts such as ether or *in vivo*, because ether that was not detected in early *in vitro* physical experiments is amplified in biological surface-tension *in vivo* systems to a level that cannot be

neglected. These are the fundamental differences between energy levels (which omit the rotational-zeroing function of the surface-tension region) and entropy levels (which do not omit the rotational-zeroing function of the surface-tension region and are regulated by the Le Châtelier effect).

Above we discussed the physical descriptive difference between entropy levels and energy levels. Below, using the simple melody Twinkle, Twinkle, Little Star, we can see the difference in the dynamic process of these quantum operations. The opening phrase of the melody is as follows (only with Chu's constant pitch, others such as duration, beat, etc. are omitted here):

Melody:	**C**	**C**	**G**	**G**	**A**	**A**	**G**	**F**	**F**	**E**	**E**	**D**	**D**	**C**
accompaniment:	?	?	?	?	?	?	?	?	?	?	?	?	?	?

If the melody is regarded as a quantum state, then according to the quantum-mechanical state-superposition principle $|\psi\rangle = \sum c_i |i\rangle$, to strengthen this quantum state we can only repeat the melody once or multiple times according to the energy-conservation method, producing the following result. (Because this postulate assumes that only constant-multiple linear superposition can preserve the original quantum state, the melody can only be repeatedly duplicated by a constant multiple ($\times \mathbf{C_i}$); a dot above the melody indicates an octave higher. To date, quantum mechanics has only the translational zeroing state superposition principle, without alternative *EP* rotational zeroing cache available.)

Melody	**Ċ**	**Ċ**	**Ġ**	**Ġ**	**Ȧ**	**Ȧ**	**Ġ**	**Ḟ**	**Ḟ**	**Ė**	**Ė**	**Ḋ**	**Ḋ**	**Ċ**
accompaniment:	C	C	G	G	A	A	G	F	F	E	E	D	D	C

(*Energy-conservation accompaniment, repetitive melodic superposition by a constant($\times \boldsymbol{C_i}$) following the classical translational-zeroing* ***quantum-state postulate****;* ***no EP/inversion-intaking cache*** *is available.*)

However, such an operation leaves no cache for intaking *EP*. If we look at the practice of music over several centuries, the melody is not directly repeated and superposed; instead, the melody is inverted according to harmony and then superposed. Consider the simplest triad accompaniment:

Melody	**C**	**C**	**G**	**G**	**A**	**A**	**G**	**F**	**F**	**E**	**E**	**D**	**D**	**C**
accompaniment:	E	G	C#	E	C	F#	D	A	C	G	B	G	D	C

(Entropy-preservation accompaniment, inversion before superposition following the rotational-zeroing Le Châtelier's ***spin inertia****,* ***sustained by EP*** *— here, EP* ***converges the rotational zeroing*** *of melody and accompaniment by diverse musical* ***rest****.)*

The first accompaniment note is no longer the repeated C but becomes E, the first inversion of the triad; the second note is also not the repeated C but becomes the second-inversion G. The following notes proceed in the same way, always inversion before superposition, satisfying the Le Châtelier effect or $\boldsymbol{n_k = n_{k+1} + |EP\rangle}$. In particular, the # appearing in the example is a rotational-zeroing **CvS operator** originating in music, with the **terminology of "operator"** inspired by the mathematical operator formalism of quantum mechanics, but readily applicable to bio-systems. Because the CvS E-F and B-C are not located at the center of the scale, the superposition is asymmetric. Therefore, during chord inversion, to maintain this asymmetric-superposition property, or the stability of CvS (the stability of interval distances among inversions), one can only use the **CvS operators** such as sharp (♯), flat (♭), and natural (♮). Using these operators constitutes real rotational zeroing; without them, the operation remains translational zeroing. The energy-conservation compositional method described above, in which quantum mechanics simply repeats the melody, is still translational zeroing without *EP*(the quantum-state superposition principle itself is a typical translational-zeroing principle). By contrast, inversion/spin inertia or the method by which a superfluid intakes *EP*, strengthens the quantum state by taking in *EP* through rotational zeroing that maintains the corresponding CvS range. The more zeroing levels (CvS) there are, the more *EP* is taken in. CvS is a fingerprint specific to inversion/spin inertia in unsymmetric quantum superposition; symmetric quantum superposition has no such feature.

Although the asymmetric CvS-operator concept originates from music and is inspired by the Hilbert-space symetric operator formalism of conventional quantum mechanics, it is not merely a musical construct: **life itself can be understood as a natural spinal-vector CvS operation**, in which multilevel CvS operators stabilize irrotational-entropy inversion/spin inertia through the physical rotational-zeroing processes intrinsic to life. (Historically, if Schrödinger's cat is considered using the linear-superposition method of traditional quantum mechanics, it is difficult to recognize the defect. But if one could use the musical method of **inversion before superposition**, or **CvS-stablized superposition**, then a dead cat and a live cat could not be superposed because their CvS (degree of converging) differ greatly. Schrödinger's cat was the first thought experiment that in an era lacking asymmetric rotational-zeroing tools, to sense the defect of pseudo-zeroing superposition of quantum-mechanical states (note: Albeit that classical quantum mechanics established the concept of spin and the spin quantum number (m_s), its state-superposition principle has nothing to do with the **spin inertia** we introduce here. **Classical quantum mechanics does not involve spin inertia at all due to its underlying symmetry/supersymmetry; consequently, its energy levels have no CvS characteristic of rotational zeroing**).

In this section, we use the musical concept of a chord to describe inversion/spin inertia. If one insists on finding the closest mathematical-physical tool in traditional physics, a chord could be regarded as a kind of quantized torsion. The torsion employed in the Einstein–Cartan framework is continuous; had this theoretical framework attempted to introduce quantized torsion, it might have provided the closest physical analogue to a musical chord and potentially led earlier to the **superfluid rotational-zeroing quantized torsion** introduced here (despite the intrinsic difficulty of obtaining analytical solutions to Einstein's field equations, introducing quantized torsion might have provided an alternative route that could have arrived earlier at a similar result—the replacement of tissue-specific regulation by Le Châtelier weighting regulation under the spinal vector *in vivo*).

1.62 Ancient Physical Rotational-Zeroing Spinal CSF Radius Practices and Non-simultaneous Time

From Newtonian classical mechanics to relativity and quantum mechanics, physical laws possess a high degree of time-reversal symmetry under coordinate time. At the same time, the energy-conservation parameter, as temporal translational zeroing, also holds strictly within this rigid-time framework. More importantly, the superposition of time, whether quantized or non-quantized, is absolutely s**ymmetric superposition**. However, the non-simultaneous time used by bio-systems (based on rotational zeroing) is asymmetric, and the process of superposing this time is also asymmetric superposition (using two-fluid data: $\boldsymbol{T} + |\boldsymbol{T}'\rangle$, rigid time is in the T term whereas non-simultaneous time is in the $|\boldsymbol{T}'\rangle$ term). This individualized rather than global concept of time itself appeared only in modern times, but ancient China had already used specific zeroing methods of this time concept in kungfu practices. Below we examine how ancient Chinese practitioners increased rotational zeroing through physical training to prolong life, thereby allowing a better understanding of non-simultaneous time. The better the convergence of rotational zeroing of spinal CSF superfluid, the more stable the rotation; the more stable the rotation, the more *EP* non-simultaneous time it can intake from an environment, that is, the longer the lifespan. In this sense, the spinal vector provides the macroscopic organizing axis of the natural CvS operation of life, along which multilevel CvS operators continuously perform rotational-zeroing adjustments. (Thousands of years ago, ancient China began to apply the concept of spinal CSF **rotational-zeroing radius** to describe spinal CSF stability. They even considered human obesity to result from a loose body and weak muscles, with this looseness arising because the **spinal zeroing radius** had loosened and expanded. If our present rotational-zeroing system is used, the radius used by the ancients is directly related to the extension range of CvS along the spine. The tighter the radius or the stronger the convergence, the more stable the CSF, and under the same environment the wider the extension range of the **Convergence Spectrum**. Although ancient Chinese

practitioners did not know that CvS was an upgraded version of their zeroing radius, they did, using only this lower-version zeroing radius, create two of the world's highest-level kungfu schools: Wudang and Shaolin.)

Kneeling spinal converging first appeared in the Shang dynasty. Jade artifacts from 1600–1046 BCE **(Fig. 1b①)** show this layperson posture. At first it was used only in rituals and by social elites; by the Qin dynasty (221–206 BCE) it began to spread to common people and became widely used by the entire population. It gradually disappeared only after the fall of the Qing dynasty (1912), while Japan today still retains this custom transmitted from China during the Tang dynasty (618–907 CE). This posture was used from age seven through old age. **(Fig. 1b②)** Double-cross-legged sitting is an introductory posture for professional kungfu practitioners, but at least three years of kneeling converging training is required before beginning this method (see **suppl.doc 1** of this three-year progression from layperson to professional pilot training). **(Fig. 1b③)** shows a Shaolin spinal converging practice with a history of more than 1,500 years, and **(Fig. 1b④)** shows the 600-year-old Wudang Taihe spinal converging practice (this bridge posture requires physical rotational zeroing aligned with the navel and crown hair whorl, potentially requiring decades of training; see **Suppl. Doc. 2**). These three long-standing forms of physical training use the spinal CSF converging training just described. Kneeling is rotational-zeroing lifestyle etiquette for all laypersons (ordinary lifestyles, unlike professional kungfu training, which requires certain lifestyle restrictions). It can naturally increase the converging stability of spinal CSF without requiring dedicated physical exercise time. The reason it spread throughout China for thousands of years is that, under otherwise equal conditions, ordinary people could obtain an average lifespan more than ten years longer than modern people sitting on stools merely by adopting this lifestyle, even without any special physical training. (Japan today maintains the world's longest average life expectancy, possibly related to retention of this posture transmitted from China during the Tang dynasty; the stools used in modern life may directly **affect spinal CSF** stability and, consequently, **lifespan**.) Double-cross-legged sitting is an introductory posture for professional practitioners, but requires more than three years of kneeling as a foundation. Shaolin spinal converging and Wudang converging are specialized training methods for professional practitioners. Professional training simply adds some lifestyle prohibitions compared with laypersons, but the principle is the same as kneeling. These two schools also include training similar to modern sports, such as muscle strength and striking intensity. When such training reaches a certain level, it causes deviation of the convergence spectrum along the spine. These two spinal-converging practices use rotational zeroing after routine training to adjust spinal CSF deviation back, that is, to reduce the rotational radius of CSF as ancient Chinese practitioners described, in order to achieve longevity. (Modern sports originated in the ancient Greek and Roman Olympics and did not have a similar rotational-zeroing method. Therefore, competitive sports generally have an impact on lifespan because excessive competitive training causes spinal CSF CvS deviations without an appropriate method to readjust them. The average lifespan of competitive athletes is only slightly higher than that of people who do not exercise, but is generally lower than that of ordinary noncompetitive exercisers, possibly because of the absence of a spinal rotational-zeroing training system like that of ancient China. These ancient Chinese physical-training spinal-convergence systems would be equally practical if grafted onto modern sports systems, because they fully embody the rotational-zeroing-radius mechanism of non-simultaneous time.) The term **operator** was originally introduced in translational-zeroing classical quantum mechanics to denote mathematical operation acting on a physical state. We introduce the concept of the **CvS operator** because musical composition has actively applied a rotational-zeroing framework for centuries, in which sharp (♯), flat (♭), and natural (♮) function as operators that preserve inversion/spin-inertia stability during inversion. This operational principle coincides with the **asymmetric rotational-zeroing quanta framework**. Ancient Chinese kungfu training provides a seemingly very different practice but operates through an identical physical mechanism. Although its spinal practices are substantially more complex and require decades of training, they likewise function as **spinal spin-inertia operators** through physical rotational zeroing to regulate the human body. Thus,

these apparently very different forms of rotational-zeroing implementation can reasonably share the terminology of **"CvS operator"** because they operate through the same underlying mechanism.

Modern stem-cell transplantation and organ transplantation also involve non-simultaneous time. Organs need to use the non-simultaneous time on spinal CSF. From the immune perspective, innate immunity has a small rotational-zeroing radius, whereas acquired adaptive immunity has a large rotational-zeroing radius. Even if a native organ has problems, it remains associated with the core portion of rotational zeroing. A transplanted organ, even the best-matched organ removed from a living donor, can still occupy only the peripheral portion of rotational zeroing. This means that the core portion must regenerate a substitute organ component before survival is possible, and this process has a major impact on lifespan. At present, the survival period after organ transplantation is in most cases not long, because the transplanted organ does not match the host spinal CSF zeroing radius/CvS, causing the rotational radii of the organ and CSF rotational zeroing not to converge. Stem-cell transplantation is the same. Many cells can grow into muscle *in vitro*, but when placed at a site of muscle injury for regeneration, they still cannot regrow muscle; this is also a problem of the spinal CSF rotational-zeroing radius or CvS. Therefore, stem-cell or organ transplantation can only barely be regarded as compromise approaches for treating disease and cannot become approaches for improving health level. Any genuine health approach rather than disease treatment—whether physical exercise, consumption of foods or health products, or even hospital disease treatment—must withstand verification by our human ***FHD*** method when comparing before and after treatment. This is currently the only known effective positively correlated health indicator (the higher the measured value, the higher the individual health level), with no alternative detection method.

1.63 Shifting of gravity/Planck constant

Since non-simultaneous time represents the degree of *EP* stability of rotational zeroing, it is not difficult to understand that the gravitational constant and Planck constant shift under this type of time. We have already derived from gravitational two-fluid data $\boldsymbol{G_{gravitational} = G_{Cavendish} + G'_{rotational}}$ that the gravitational constant contains not only the translational-zeroing-energy Newtonian rigid-body term $\boldsymbol{G_{Cavendish}}$, but also a rotational-zeroing-entropy term $\boldsymbol{G'_{rotational}}$; the actual gravitational constant is the combination of the two in a given environment. For ordinary nonliving objects, although the latter term $\boldsymbol{G'_{rotational}}$ is difficult to measure and is relatively small in magnitude, it remains nonzero. In bio-systems it becomes $\boldsymbol{|G'_{rotational}\rangle}$, for which Dirac notation is introduced to denote its involvement in a stable alive quantum state. The approximately 10^9-level amplification of the gravitational constant essentially originates from rotational-zeroing-living-entropy dynamics in bio-systems. For objects close to rigid bodies, where the surface-tension term $\boldsymbol{|F'\rangle}$ can be neglected, the rigid-body gravitational constant $\boldsymbol{G_{Cavendish}}$ is therefore almost unaffected by the rotational term $\boldsymbol{G'_{rotational}}$.

1.64 Mechanism of biological memory

Computer memory and most forms of memory we encounter necessarily contain coding/decoding processes. Biological memory, however, is completely different from these memory modes of coding/decoding. Biology uses rotational zeroing and *EP* Le Châtelier memory; what is remembered is asymmetric inversion entropyflow and has little relation to coding/decoding of the energy-conservation era. (Entropyflow is based on Le Châtelier reverse flow in the surface-tension region, whereas energy flow in coding/decoding is entirely forward flow based on a reference system.) Interestingly, Gauge Theory also contains the concept of a "Memory Effect" [14]. The Memory Effect refers to a nonzero change in the gauge-field configuration between the early stage ($u\to-\infty$) and late stage ($u\to+\infty$) of a scattering process, when the radiation-field strength disappears and the system returns to the vacuum state. This change can be represented as the gradient of a pure-gauge function: $\Delta A_z=\partial_z\phi(z,\bar{z})$.

Therefore, the change is essentially equivalent to the footprint left at the boundary by a large gauge transformation. However, gauge-field memory contains an irreversible change and does not involve the Le Châtelier effect or *EP*, that is, it does not involve inversion entropyflow; it is therefore actually quite different from biological memory.

Gene scissors such as CRISPR/Cas9 [15] contain a complete Le Châtelier regulatory mechanism and asymmetric rotational zeroing and are the earliest known memory mechanism at the biological genomic level; in medicine this is also called innate immunity. Its mechanism ultimately developed into the human brain. When people first dissected the brain, they wondered how the small hippocampus could store memory data. In fact, the hippocampus stores not memory data but inversion/spin inertia. Once an entropyflow passes through, inversion immediately activates other related inversions. This structure requires none of the data used in traditional coding/decoding. Environmental participation is an early physical term indicating the degree of *EP* in a rotational-zeroing system. Memory is the internal and external Le Châtelier gravitational effect under this *EP*. Superposition occurs only after inversion, and the *EP* during inversion superposition is memory. *EP* and memory overlap to a large extent. The brain–computer interfaces claimed by some people are in fact only a commercial operation and have no scientific or medical value, because an implanted chip belongs to a translational-zeroing system whereas the human brain belongs to a rotational-zeroing system, making communication between them difficult. (We may even be able to use the *FHD* method to assess the impact of an implanted chip for a health receiver.)

As stated above, what Einstein pursued in his later unified-field theory was a reference that eliminated the observer effect. Under translational-zeroing conditions, the Einstein tensor no longer involves a reference frame and thereby achieves the purpose of eliminating the observer effect. Einstein did not complete the elimination of the observer effect in rotational zeroing in his later years. For bio-systems, the spinal vector and peripheral structure jointly exist within a surface-tension region; in fact, this spinal vector serves as a reference without an observer effect for the entire system under surface tension, a structure that locally eliminates the observer effect. Different parts of the biological body are regulated by the spinal vector through entropy preservation, and rather than being governed by the "**observer effect**" or tissue-specific regulation of any location, they are distinguished only by the different "weights" of the Le Châtelier effect on the spinal vector. If Einstein's pursuit had succeeded, it should have produced a model similar to the spinal vector. (Regarding this **replacement of tissue-specific regulation by Le Châtelier weighting** under the spinal vector rotational zeroing, one example can be given. Tumor tissue and normal tissue should originally be **distinguished** by their **Le Châtelier weights**. Once this **weighting distinction** disappears, both tissues are recognized by the body as the same *in vivo* structure and incorporated into the supply of irrotational entropy. This is also the fundamental reason cancer is difficult to treat. Unless normal spinal-vector regulation distinguishes the **Le Châtelier weight** of tumor cells from that of normal cells—or, in rotational zeroing, directs tumor cells outward while normal cells move toward the inner layer—it is technically impossible to solve the problem of tumor recurrence. Listening to music actually follows the same mechanism: through the auditory organs, the effects of pleasant sounds move toward the inner layers along the spine, whereas those of unpleasant sounds move toward the outer layers.)

2. Experimental consolidation of Rotational Zeroing Le Châtelier term $|F'\rangle$ from Newton's Law of Unversal Gravitation

All of the preceding discussion is essentially based on the rotational-zeroing $|F'\rangle$ term in gravity. We therefore experimentally verify this term.

2.1 Previous Experiments and the Present Physical Experiments

In 2020, we conducted a series of preliminary *FHD* experiments [10]. Most focused on the gravitational amplification between bio-systems and non-living beings and its underlying internal-motion origins. In particular the half-filled water and oil-bottle experiments, further revealed that this gravitational amplification has a surface-tension origin—namely the **inversion (turnover)-round gravitational effect**. This effect arises from the difference in turnover rounds between the surface-tension and non-surface-tension regions during free fall, which constitutes the basis of *FHD*.

The experiment first compared a half-filled bottle of water with a completely filled bottle of water. The completely filled bottle reached the ground first. Here, the full bottle did not land because of its greater weight; rather, filling the bottle restricted the number of turnovers between the surface-tension and non-surface-tension regions of the water. This was further examined by comparing a half-filled bottle of oil with a half-filled bottle of water. When simultaneously released from a height of 7.04 m, the lighter oil bottle **(173.274 g) reached the ground before the heavier water bottle (184.125 g)**, with Δ*FHD*=21.75 cm. Over the following years, we repeatedly reproduced this result at multiple locations worldwide. The results are the same, completely opposite to that of the legendary **Galileo's Leaning Tower of Pisa experiment** (claimed to have conducted in 1589–1591). Through these persistent repeated experiments, we gradually came to understand the **two-fluid data structure** of gravitation and its $|\boldsymbol{F'}\rangle$ term. While the half-filled water-bottle and oil-bottle experiments have provided considerable insight into the underlying mechanism, the present study moves beyond them by directly employing water and oil droplets to further consolidate the experimental evidence for the $|\boldsymbol{F'}\rangle$ term.

The experiments were conducted under windless conditions at a release height of **10.59** m and an ambient temperature of approximately 18°C. Water and oil droplets were simultaneously released using disposable plastic droppers (0.2 mL dropper size for oil and 0.3 mL dropper size for water, since using the **same** dropper for both liquids would not produce a sufficiently distinguishable difference in droplet weight), which were held stationary for more than 30 seconds prior to each release. Following release, the masses of the water and oil droplets were determined using an analytical balance. Ground-scale readings were obtained from photographic images, from which millimeter-scale values were extracted. The release height was measured with a laser distance meter. The water used was commercially bottled drinking water, purified through activated carbon filtration to remove chlorine. The oil was commercially available edible rapeseed oil purchased in China. Assuming the droplets to be approximately spherical, their radii were calculated from the measured masses using the respective reference densities, ρ_{oil} = 0.915 g/cm³ and ρ_{water} = 0.9986 g/cm³, according to

$$r = \left(\frac{3m}{4\pi\rho}\right)^{1/3}$$

where m is the measured droplet mass and ρ is the corresponding liquid density. *FHD* values were determined via high-speed photographic imaging. The results are presented below.

Table 1. *FHD* measurements for paired water and rapeseed-oil droplets

	FHD (cm)	$\text{Mass}_{\text{water drop}}$ (g)	Calculated $\text{Radii}_{\text{water drop}}$ (mm)	$\text{Mass}_{\text{oil drop}}$ (g)	Calculated $\text{Radii}_{\text{oil drop}}$ (mm)
1	34.3	0.0247	1.807	0.0177	1.665
2	28.7	0.0223	1.747	0.0139	1.536
3	36.5	0.0229	1.762	0.0153	1.586
4	45.1	0.0211	1.715	0.0141	1.544
5	37.2	0.0245	1.803	0.0165	1.627
6	41.8	0.0268	1.857	0.0188	1.699
7	30.5	0.0232	1.770	0.0132	1.510
8	39.6	0.0216	1.728	0.0166	1.630
9	43.2	0.0214	1.723	0.0184	1.687
10	32.3	0.0209	1.710	0.0149	1.572
11	38.9	0.0190	1.656	0.0170	1.643
12	44.7	0.0223	1.747	0.0133	1.514
13	31.4	0.0207	1.704	0.0157	1.600
14	40.8	0.0191	1.659	0.0181	1.678

15	35.9	0.0195	1.671	0.0145	1.558
16	42.5	0.0178	1.620	0.0168	1.637
17	29.6	0.0232	1.770	0.0132	1.510
18	37.8	0.0226	1.755	0.0176	1.662
19	40.2	0.0234	1.775	0.0154	1.590
20	34.7	0.0190	1.656	0.0180	1.675
21	43.9	0.0179	1.624	0.0149	1.572
22	33.1	0.0223	1.747	0.0163	1.620
23	39.4	0.0177	1.617	0.0137	1.529
24	36.8	0.0181	1.630	0.0171	1.646
25	42.0	0.0235	1.778	0.0155	1.593
26	30.9	0.0178	1.620	0.0188	1.699
27	41.3	0.0252	1.820	0.0142	1.547
28	35.2	0.0266	1.853	0.0164	1.623
29	38.5	0.0234	1.775	0.0136	1.525
30	44.3	0.0223	1.747	0.0172	1.649
Ave	37.703	0.021693	1.728	0.015890	1.604
SD	4.839	0.002616	0.0699	0.001774	0.0600
RSD	12.83%	12.06%	4.05%	11.16%	3.74%

These results again consolidate the observation that the lighter oil droplets reached the ground before the heavier water droplets, contrary to the result attributed to Galileo's experiment and consistent with our previous experiments using half-filled water and oil bottles. Quantitatively, the mean water-droplet mass was 36.5% greater than the mean oil-droplet mass (0.021693 vs 0.015890 g), whereas the calculated mean water-droplet radius was only 7.7% greater (1.728 vs 1.604 mm). No meaningful linear correlation was observed between *FHD* and either droplet mass or calculated radius (Pearson $r = -0.042$ and -0.047 for water mass and radius, respectively; $r = 0.114$ and 0.117 for oil mass and radius, respectively; $|r| \leq 0.12$). The estimated Stokes drag was only ~4% of gravity. Thus, within the present experimental analysis, the observed ***FHD*** cannot be accounted for by droplet mass, calculated radius, or estimated air resistance, and instead **represents a systematic difference (**dynamic interlayer viscosity between surface-/non-surface tension region**s) between the water -/ rapeseed-oil droplets**.

In the conventional law of universal gravitation, the Newtonian rigid-body term $\boldsymbol{F} = G\frac{Mm}{r^2}$ acts downward. In contrast, the resultant force associated with the rotational-zeroing surface-tension Le Châtelier term $|\boldsymbol{F}'\rangle$, which is sustained by *EP*, acts in a direction that reduces the effect of $\boldsymbol{F}$; its net effect is therefore opposite to the downward $\boldsymbol{F}$. The effect of this surface-tension term $|\boldsymbol{F}'\rangle$ comes from the rotational **interlayer coupling** (or *EP* intaking **dynamic-interlayer-rotational-viscosity**) between the surface-/non-surface-tension regions during free fall (the dewdrops rolling on leaves are maintained by this $|\boldsymbol{F}'\rangle$ term rotational interlayer coupling tendency, whereas the $\boldsymbol{F}$ term actually acts to disperse the drops; even in more complex biological systems, aging still simply corresponds to the gradual weakening of such rotational interlayer coupling effects, or more accurately, to the weakening of *EP*-uptake capacity between the rotational-coupling layers. Whether in simple water/oil droplets or in complex living cells, the system can be conceptually divided into a surface-tension region and a non-surface-tension region. The horizontal Le Châtelier effect occurs mainly inside the surface-tension region, whereas the vertical Le Châtelier response between the two regions is inseparable from it. When an external perturbation produces a displacement between the two regions, their coupled Le Châtelier responses in both directions tend to restore them toward their original relative configuration by taking up *EP*. The strength of this interlayer coupling, or the capacity to take up *EP* to restore the two regions, therefore provides an underlying indicator of aging). The difference observed between oil and water droplets is a consequence of the different rotational interlayer coupling between these two regions, **as further supported by the quantitative analysis in Table 1 showing that the observed *FHD* cannot be accounted for by droplet mass, calculated radius, or estimated air resistance.** As in the half-filled water versus half-filled oil experiments, the interpretation in **Table 1** is also supported by the pilot experiment comparing a half-filled water bottle with a completely filled water bottle, in which the latter hit the ground first; as well as by the bi-layer metal-ball experiments, in which interlayer oscillations increased *FHD* [10].

For the Newtonian rigid-body $\boldsymbol{F}$ term examined in the legendary Galileo Leaning Tower of Pisa experiment to produce simultaneous landing, two conditions are required: first, the falling objects must be solid metal balls approximating rigid bodies, such that the influence of $|\boldsymbol{F}'\rangle$ term is small; second, the falling objects must **remain non-rotating during the fall** (the translational Newtonian result $t = \sqrt{2h/g}$ holds only when ω=0. This non-rotating requirement is practically challenging for objects released by human hands from the 55 m Leaning Tower. It should be recognized that although the rotation of solid metal balls during free fall does not exhibit the multi-layered, non-uniform rotation observed in water/oil droplets, such rigid-body rotation during free fall still has a very substantial effect on the outcome of simultaneous landing). In our oil / water-droplet experiments, first, the effect of the $|\boldsymbol{F}'\rangle$ term is much greater than that of the $\boldsymbol{F}$ term. Second, the non-simultaneous rotation of the oil/water droplets during free fall is inevitable, even though they have been stabilized for 30 s before release. The observed *FHD* therefore arises from differences in the degree of rotational-zeroing interlayer coupling between the surface-tension and non-surface-tension regions of the oil/water droplets. As nonliving systems evolved into complex cellular life, the growth/aging cycle of a cell, regardless of species or evolutionary level, remained governed by the same rotational-zeroing interlayer coupling between surface-tension and non-surface-tension regions. The only difference is that, in living systems, the surface-tension regions have become highly folded, whereas non-surface-tension components are excluded through quantum gravity rotational zeroing and discharged as waste.

From here, we can understand that various signaling pathways involved in biological development, such as **Wnt/β-catenin** and the **PI3K/AKT/GSK-3β signaling axis**, are typical examples of such $|\boldsymbol{F}'\rangle$ term Le Châtelier effects extending from the cell nucleus toward the membrane surface. The currently recognized processes of membrane–nucleus communication, including reciprocating movement from the nucleus toward the membrane, involve numerous known signaling pathways [16]. However, their underlying mechanism does not primarily depend on the catalytic actions of enzymes or transporter proteins as claimed by modern biology; these claims can only be secondary. The primary physical mechanism proposed here is instead the driving action of the $|\boldsymbol{F}'\rangle$ term revealed by the present free-fall experiments with water and oil droplets. This rotational zeroing *EP* interlayer driving force is a natural function of the surface-tension region in both non-living water/oil droplets and living cells, with biological evolution amplifying its magnitude beyond that observed in non-living systems—a gravitational amplification whose empirical basis is the very **spin inertia *CvS*** demonstrated in our water-/oil-droplet experiments. In essence, *FHD* and flow-cytometric **cell sorting** share the same underlying physical mechanism, as both partitioning dynamics arise from the same quantum-gravity **rotational-zeroing interlayer coupling between the surface-/non-surface-tension regions** of the targets. The physical **water-zeroing** (or *in vivo* water-asymmetric-distribution) problem discussed later reflects the **elasticity of living cells** and is governed by this same rotational interlayer coupling mechanism. This also explains why liquid-nitrogen preservation can maintain cells only for a limited period: extremely low temperatures eventually impair the cells' ***in vivo*** **interlayer coupling elasticity**, constituting a form of low-temperature **storage aging**.

More generally, it is noteworthy that, in the era of thermodynamics and energy conservation; it is a common sense that solutes diffuse from regions of higher concentration toward regions of lower concentration. In bio-systems, numerous forms of uptake proceeding against thermodynamic gradients have been observed. To reconcile such observations with this conventional understanding, biology invoked a variety of enzymes, transport proteins, etc., effectively endowing them with a seemingly "supernatural power" to drive anti-thermodynamic-gradient motion. What was not recognized is that Le Châtelier motion against a thermodynamic gradient is itself a natural function of the surface-tension term $|\boldsymbol{F}'\rangle$, rather than a property unique to living systems; accordingly, such motion does not intrinsically require enzymes or transport proteins as its fundamental driving mechanism. Therefore, the conventional assumption that solutes necessarily diffuse from higher to lower concentrations ceases to hold, even in non-living systems, wherever the surface tension term $|\boldsymbol{F}'\rangle$ exceeds a critical threshold.

2.2 A Stable *FHD* Measurement Method Using the $|F'\rangle$ Term for Human Innate Health Assessment

In our previous work, *FHD* was used to assess human health and food freshness [10]. Existing clinical indicators used in hospitals are primarily disease indicators—that is, indicators used to determine whether medical treatment is required. For individuals who are considered not to require treatment according to these indicators, no further differentiation is generally made. *FHD*, by contrast, is a health indicator intended to assess characteristics such as innate immune capacity and the degree of development/aging. Among individuals who are considered not to require treatment according to existing hospital criteria, *FHD* can further distinguish those with different levels of health. To the best of our knowledge, it is the only existing indicator of this kind, and it may reflect the sensitive range of all remaining disease indicators under specific conditions.

When the 10-m commercial diving platform *FHD* test was first introduced on at the Etobicoke Olympium, the testing method was not yet fully developed. We now provide a standardized method subsequently developed to obtain stable *FHD* measurements for fundamental research and potential population-level application. The procedure is illustrated in (**Fig. 1c)**: ① sit at the edge of the 10-m diving platform while holding the thighs and keeping the lower legs flexed; ② extend the lower legs forward to shift the center of gravity, allowing the body to fall naturally from the platform; and ③ minimize unnecessary movements throughout the procedure and enter the water in an upright position. This approach yields stable *FHD* measurements (to obtain *FHD* measurement stability, diverse athletic diving manoeuvres must be avoided).

This *FHD* health indicator can first reflect sleep. Sleep can be regarded as a process through which part of the chaotic entropy generated by spinal activity during the daytime is restored through *EP* into irrotational entropy. *EP* intake during daytime activity and *EP* intake during nighttime sleep differ in their oscillation ranges and intensities, or, equivalently, in the periods of quantum-gravitational non-simultaneous time that they generate. Thus, an individual's *FHD* value reflects not only innate immune capacity and the degree of aging/development, but also directly reflects sleep quality. For the same individual under the same environmental conditions, periods with higher *FHD* values (longer free-fall suspension times) necessarily correspond to periods of better sleep quality. With increasing age, the *FHD* value approaches that of non-living objects, while sleep duration becomes progressively shorter. Measurement of sleep quality using *FHD* values is highly reliable, and currently no alternative measurement method is available. Our reservations regarding organ transplantation also arise from this consideration. In animals undergoing organ transplantation, both *FHD* values and sleep quality are severely affected after surgery, indicating that this technology has difficulty improving health status and can only extend survival for a limited period in individuals near death. Death, in this framework, is the state in which chaotic entropy can no longer be transformed via *EP* into irrotational entropy, or, equivalently, in which non-simultaneous time can no longer be generated.

In addition to reflecting sleep quality, *FHD* values also reflect the degree of aging associated with food-absorption efficiency. During the Copenhagen era of quantum mechanics, spin-up and spin-down were considered to undergo spooky collapse entanglement because surface-tension effects were omitted. In the digestion, sweetness corresponds to spin-up and saltiness to spin-down. The conversion cycle between these two rotational states can extend to approximately 24h, and the degree of youth or aging of an individual depends on the efficiency of this spin-up/spin-down conversion. Younger individuals intake more *EP* during this conversion, whereas aging individuals intake progressively less *EP*. *FHD* values therefore also reflect aging-related efficiency of food digestion. The use of *FHD* values to assess the degree of aging across other forms of human activity can ultimately be regarded as rooted in these two fundamental physiological functions: **digestion and sleep**. In essence, *FHD* measures **spinal spin inertia**. (The above model in which sweetness corresponds to spin-up and saltiness to spin-down has a history of more than 2,000 years in ancient Chinese practice. Thus, although the associated theoretical framework was only recently completed, its practical application has a long standing history.)

2.3 Macroscopic Water Rotational Zeroing and Microscopic Molecular Rotational Zeroing: The *FHD* Mechanism

To understand the physical mechanism underlying *FHD* measurement, we further examine the problem of **macroscopic water rotational zeroing in feces formation**. Modern biomedicine has constructed extensive chemical and nutritional descriptions of how feces are formed, involving saliva, gastric juice, pancreatic juice, bile, intestinal fluid, the large intestine, and other components. Approximately twenty to thirty major enzymes participate in digestion; when isoenzymes and subtypes are included, the total may exceed forty, even without counting enzymes secreted by intestinal microorganisms. Faced with such a complex molecular inventory, even specialists outside this particular field may find it difficult to name all of these enzymes. Yet these bundles of descriptions still do not directly answer a more fundamental question: **how exactly are feces formed?** At the physical level, feces formation is simply a problem of **physical water zeroing**. The entire digestive process can be expressed in a **two-fluid-data** format of rotational zeroing: **liquid + solid**. Suppose that the liquid phase has one rotational center and the solid phase has another. If the radii of the two centers are properly close to produce convergence, normal feces are formed. Excessive deviation of the liquid center results in diarrhea, whereas excessive deviation of the solid center results in constipation. Regardless of the evolutionary level of a species or the enormous differences among living environments, feces formation is fundamentally such a simple physical problem of **water rotational zeroing**.

As for the various chemical and nutritional models of modern medicine described above, all of them must be secondary to this physical problem of water rotational zeroing; without basing on this physical water-zeroing model, they become ineffective. It should be noted that the **physical rotational zeroing of water** described here is not the removal of water by centrifugation, as in the energy-conservation paradigm. Its driving force originates from the **spin-inertia** generated by the rotational-zeroing superposition of all metabolic cycles in the body. These processes require *EP* and are unrelated to the centrifugal removal of water; a centrifuge cannot intake *EP*, whereas for spin inertia CvS, each metabolic cycle does require *EP*. This simple physical water zeroing also presents an extreme challenge for synthetic biologists. Whether in the pathways of biological growth, evolutionary activity cycles, or water zeroing itself, many of the steps require *EP*. Modern technology has made it possible to assemble short DNA fragments into larger constructs, and even to synthesize proteins or replace large cellular tissues. However, none of these artificial manipulations can introduce *EP*. This is precisely why obtaining a product with genuine bio-activity remains extremely difficult—the bottleneck lies not in DNA sequences, protein structures, or cellular architecture,etc., but in the absence of *EP*. Here, *EP* can be simply understood as an *in vivo* physical water zeroing condition that still remain insurmountable for modern bio-technologies. Every step *in vivo* involves *EP*, meaning that the physical water zeroing of individual genes is coupled through *EP* to genome-wide cellular or even somatic water zeroing. In contrast, artificial gene editing is fundamentally based on local manipulation. Even if local water conditions can be altered after editing by means such as centrifugation, such localized changes remain disconnected from the overall genomic water condition. Consequently, the CRISPR/Cas9 concoction remains constrained by the global water condition. Thus, what appears to be a simple **water-condition/*in vivo*** elasticity requirement is, for synthetic biologists, effectively insurmountable.

Modern organ transplantation still faces essentially the same water zeroing technical barrier. Modern medicine often gives the misleading impression that the **sole obstacle** to stem cell/organ transplantation is immune compatibility—hence the proliferation of various immunosuppressive techniques, and even genetically engineered xenotransplantation. Yet for all their sophistication, none of these approaches are capable of addressing a simple **physical water zeroing** requirement: whether the transplanted tissues or organs are consistent with the recipient's own physical water zeroing condition. The cost of such inconsistency, in terms of its impact on lifespan, is immense. Modern medicine, and even the

whole scientific community, currently even has no way to determine the **physical water zeroing** condition of a given biological sample except through long-term *FHD* data. Such a detection method can hardly be applied to an organ that is about to be transplanted (while assessing organ water-zeroing condition via *FHD* is methodologically identical to *FHD* food freshness (= *in vivo* water content/elasticity) evaluation, it is substantially more challenging due to the stringent requirement for non-destructive sample preservation).

Regarding how life evolved, Miller conducted experiments simulating the production of biological molecules by lightning under conditions intended to represent the primitive Earth [17]. However, after these macro-molecules were produced, how did they subsequently evolve into life? Numerous explanations have been proposed, including the story of an **RNA world** [18]. In fact, after amino acids and other biological molecules were formed through such lightning processes, the next stage still involved a macroscopic physical water-zeroing problem similar to the feces-formation process described above. These primordial terrestrial biomolecules likewise had to undergo prolonged evolution toward appropriate **rotational-zeroing axial distances or spinal-vector CvS** before biological activity could emerge. The RNA-world hypothesis for the evolution of life was proposed on the basis of the role of RNA in transmitting DNA-encoded information within living organisms. However, that represents a condition after the cell rotational zeroing system had already been established and does not demonstrate that the same sequence necessarily occurred during the zeroing of primordial macromolecules. A more reasonable explanation is that RNA and DNA belong to the same level of physical water zeroing, and there is no reason that one must have arisen before the other under primordial environmental conditions. RNA has also been found to participate in protein synthesis at the membrane, substantially revising the traditional conclusion that RNA/DNA processes occur in the cytoplasm [19]. According to our two-fluid data model, such a revision is more consistent with **Le Châtelier rotational zeroing $|F'\rangle$ term**. More importantly, we should also recognize that traditional biology merely describes life as requiring drinking water, air, food, and other necessities. These, however, are only secondary external manifestations. More fundamental is the continuously sustaining by *EP*: the loss of *EP* by any living system is equivalent to immediate death, whereas a living organism deprived of specific necessities such as drinking water, air, or food can still survive for a certain period (a fact underscored by modern biotechnology's failure to bridge the barrier between drinking water and *in vivo* water. We should carefully recognize that drinking water can operate under symmetric rigid time, whereas *in vivo* water must be continuously sustained by *EP* asymmetric non-simultaneous time).

Once we review both the **macroscopic water-zeroing problem of feces formation** and the **microscopic water-zeroing problem among biomolecules**, we can understand why *FHD* can effectively measure **non-simultaneous time**. From the macroscopic to the microscopic scale, the entire bio-system undergoes physical water rotational zeroing and follows **quantum gravity spin-inertia CvS**, **thereby functioning as a multilevel natural spinal-vector CvS operation.** During free fall, *EP* acts through the highly folded somatic surface-tension regions, thereby enabling *FHD* measurement with enhanced sensitivity. *FHD* therefore constitutes a reliable indicator of ***in vivo*** **water content, cellular or somatic elasticity, and aging** (these three terms are equivalent for *FHD* measurements), fundamentally different from the diverse disease indicators used in medicine.

3. Applicaton of Rotational Zeroing Convergence Spectrum into Bio-systems

3.1 Previous Physical Experiments Demonstrating the $|F'\rangle$Term and Bioinformatic Evidence for Rare-Codon Rotational Zeroing

In our previous work, we conducted extensive Cavendish mutation/*FHD* experiments [10]. In the present experiments, oil and water droplets were used to further verify the $|F'\rangle$ term in the law of universal gravitation.

In addition, in our previous bioinformatic study, rare codons were analyzed across eight species [1]. The results demonstrated that, from the relatively simple *E. coli* to the most highly evolved organism, humans, rare codons are generated through rotational zeroing, because only rotational zeroing can produce a uniform distribution of rare codons. At that time, **Table 2** presented only the genome-wide evidence for rare-codon rotational zeroing. In fact, we also performed numerous local rare-codon analyses in these eight species—for example, separately extracting respiratory chains and photosynthetic chains—and obtained similarly well-distributed rare-codon patterns. Although these local results were not published, they likewise demonstrated that rare codons are generated entirely through rotational zeroing rather than through so-called random mutations. Since rare codons are generated through rotational zeroing, they must possess characteristic CvS, with these spectra steering the movement of rare codons.

Table 2. Rare-Codon Linearity Shift with Respect to CDS Length Across Eight Species [1]

Species	Data Source	CDS Count	Total Codons	Rare Codons (12–24‰)	Pearson r	Slope
E. coli	GCF_000005845.2	4,318	1,342,295	23	0.991	0.413
Salmonella enterica	GCF_000006945.2	9,108	2,863,442	23	0.990	0.402
Saccharomyces cerevisiae	GCF_000146045.2	6,008	2,933,521	28	0.991	0.479
Phaeodactylum tricornutum	GCF_000150955.2	10,412	4,845,171	42	0.998	0.716
Brassica napus	Uploaded dataset	96,440	38,258,366	21,528,621	0.995	0.570
Danio rerio	GCF_049306965.1	89,854	~11,200,000	22–23	0.995	0.569
Mus musculus	GCF_000001635.27	98,005	66,614,578	33	0.994	0.557
Homo sapiens	GCF_000001405.40	146,337	99,625,497	32	0.992	0.533

We should recognize that although the technical capabilities of traditional molecular genetics have advanced enormously since the Newtonian era, its theoretical methods still essentially employ the **translational zeroing** inherited from that era. In reality, however, almost all biological processes, including signaling pathways, follow **rotational-zeroing regulation**. Biology therefore faces the necessity of introducing rotational zeroing into its theoretical framework. To make such updates possible, the first requirement is to identify the **fingerprint of spin inertia—CvS**. In this framework, biological regulation can be viewed as the execution of multilevel CvS operators within the overall spinal-vector CvS operation of life. We should also recognize that symmetric energy-conservation quantum mechanics initially relied on mathematical tools to predict atomic spectral lines, such as those described by the Balmer and Rydberg formulas. The spectral lines themselves do not exhibit convergence or divergence, and these spectral lines were obtained through experimental observation rather than statistical methods (spectral lines should be eigenstates rather than mixed quantum states). In the asymmetric **entropy-preservation** model, however, CvS intrinsically entails a converging process; therefore, statistical methods must be employed from the outset to detect this **converging action**. It should also be noted that atomic spectral lines do not exhibit aging behavior, whereas **CvS** in biological systems does indeed have its own **aging cycle** (the entropy-level spectrum is considerably more intricate: CvS forms the strong converging bands, whereas Chu's constant forms the weak converging bands. The intervals between these weak bands vary with the state of the system, rather

than being represented merely in terms of probabilities of occurrence, as in the conventional quantum-mechanical description, **aging** here means a progressive **weakening of the converging capability** or the **de-quantization of the spinal vector.** Here, CvS functions as a rotational-zeroing counter: irrespective of the tissue from which a rotational-zeroing event originates, it is naturally counted into the spinal vector. This counting function provides the statistical basis for detecting CvS). We should carefully note that the conventional energy-level spectrum may also be interpreted as an occurrence spectrum rather than as a direct record of every individual electronic transition. We should carefully note that the conventional energy-level spectrum may also be interpreted as an occurrence spectrum rather than as a direct record of every individual electronic transition. Accordingly, $\boldsymbol{E=h\nu}$ characterizes the energy of the radiative quantum when photon emission occurs, but should not by itself be taken to imply that every electronic transition necessarily emits a photon. In the present model, **once rotational zeroing is incorporated** beyond the conventional translational-zeroing description, photon-emission events are estimated to account for less than 1% of the underlying transition occurrences; they therefore represent only a small radiative subset rather than the totality of those occurrences.

In attempting to construct CvS using rare codons, we also make use of a characteristic feature of bio-systems. As mentioned previously, there is essentially no tissue specificity within the ***in vivo*** environment; the direction of motion is determined only by **Le Châtelier weighting**. This means that whether rare codons, particular genes, a gene family, the whole genome, particular proteins, cells, or tissues are used to identify CvS, the resulting CvS should oscillate within a certain region, with relatively small differences in their positions along the **spinal vector**. This is a characteristic **converging** feature of the rotational zeroing entropy preservation paradigm, which we can employ for **CvS detection**.

A fundamental characteristic of biological membranes is **selective permeability**. This selective permeability does not originate from enzymes/transporter proteins; rather, its intrinsic underlying origin is **CvS**. Regardless of the particular structure involved, components that enhance CvS stability or conform to the dynamics of **spin inertia** are integrated into the system, whereas those that reduce this stability are expelled as waste. Within the natural spinal-vector CvS operation of life, this selection process can be understood as a membrane-level manifestation of **natural CvS operators**, which continuously adjust molecular integration and exclusion according to CvS stability and spin-inertia dynamics. This produces the externally observable selective permeability of biological membranes. Thus, selective permeability originates from **spin inertia**, rather than from the enzymatic mechanisms claimed in modern biology. This Le Châtelier-weighted selective permeability of biological membranes, which possesses **memory characteristics**, is likewise based on the physical rotational-zeroing mechanism **underlying CvS-operator dynamics**, as supported by our water-droplet/oil-droplet experiments, and contributes to the **entropy-preservation** rather than **energy-conservation paradigm**.

3.2 Preliminary *E.coli* Genomic CvS Zeroing Detection

As discussed before, musical harmonics employs **CvS operators**, namely **sharp (♯), flat (♭), and natural (♮)** to conduct **rotational zeroing** during chord inversion to preserve relevant **CvS**. We therefore extend this Convergence Spectrum-stabilized spin inertia rotational zeroing mechanism into bio-systems for evolutionary modulation, starting from *E. coli*:

3.2.1 Genome-wide Rare-Codon Density Landscape Construction

The complete coding sequence dataset of *Escherichia coli* K-12 was obtained from the reference genome **GCF_000005845.2**, containing a total of **4318 CDS sequences**. Each CDS was converted into a codon-level representation according to its annotated reading frame.

For each CDS, the nucleotide sequence was divided into consecutive codons:

$$CDS_i = (c_1, c_2, c_3, \dots\dots\ c_n)$$

where ci represents the codon at position i.

To generate a genome-wide rare-codon density landscape, a sliding-window approach was applied along each CDS. For a window size of w codons, the local density value at position x was calculated as:

$$D(x) = \frac{1}{w}\sum_{i=x}^{x+w-1} R(c_i)$$

where:

- $R(c_i)$ represents the rarity score of codon c_i;
- w represents the sliding-window size.

In the initial genome-wide screening, a **30-codon sliding window** was applied to balance local sequence resolution and statistical stability.

CDS sequences shorter than the minimum window requirement were excluded from density-landscape construction. After filtering, the remaining CDS sequences were used for genome-wide rare-codon density profiling.

The resulting density profiles provided continuous positional landscapes of rare-codon organization along individual coding sequences.

3.2.2 Rare-Codon Statistical Field

Instead of defining rare codons as a binary category, a continuous statistical representation was introduced to preserve quantitative codon usage information. The genome-wide occurrence frequency of each sense codon was calculated from the complete *E. coli* CDS dataset.

For each codon c, the codon usage frequency was defined as:

$$F(c) = \frac{N(c)}{\sum_{j-1}^{61} N(c_i)}$$

where $N(c)$ represents the total occurrence number of codon c across all analyzed CDS sequences. A continuous rarity score was then assigned to each codon according to its relative genomic usage frequency:

$$R(c) = f(F(c))$$

where lower-frequency codons receive higher rarity scores, while frequently used codons receive lower rarity scores.

Therefore, each CDS sequence: $(c_1, c_2, c_3, \ldots\ldots\ c_n)$ was transformed into a continuous rare-codon statistical field: $(R_{(c1)}, R_{(c2)}, R_{(c3)}, \ldots\ldots R_{(cn)})$

This transformation converts discrete codon information into a quantitative landscape, enabling measurement of local rare-codon density organization along individual coding sequences.

3.2.3 Draft Convergence Spectrum(DCvS) Identification: Field-to- DCvS Parameter Extraction

The continuous rare-codon statistical field generated from each CDS was further analyzed to identify local CvS regions. The rare-codon density landscape D(x) was evaluated along the entire coding sequence using the sliding-window approach described above.

Regions exhibiting locally enriched and sustained rare-codon density relative to the surrounding sequence background were identified as **Draft Convergence Spectrum (**$DCvS$**)** regions.

To avoid introducing predefined positional assumptions, $DCvS$ identification was performed based on local density characteristics rather than fixed genomic coordinates or equal-length partitioning.

For each CDS, the extracted Draft CvS region was represented by three primary parameters:

$$DCvS = (P, W, A)$$ where:

- P represents the relative position of the $DCvS$ region within the CDS;
- W represents the width of the $DCvS$ region;
- A represents the local rare-codon density intensity.

The relative position was calculated as:

$$P = \frac{x_c}{L}$$

where x_c is the center position of the identified $DCvS$ region and L is the total CDS length.

The width parameter was defined as: $W = x_{end} - x_{start}$

where xstart and xend represent the boundaries of the identified density-enriched region.

The density intensity parameter was derived from the local rare-codon density value within the $DCvS$ region.

Therefore, each CDS was converted from a nucleotide sequence into a preliminary CvS representation consisting of positional, spatial, and intensity characteristics.

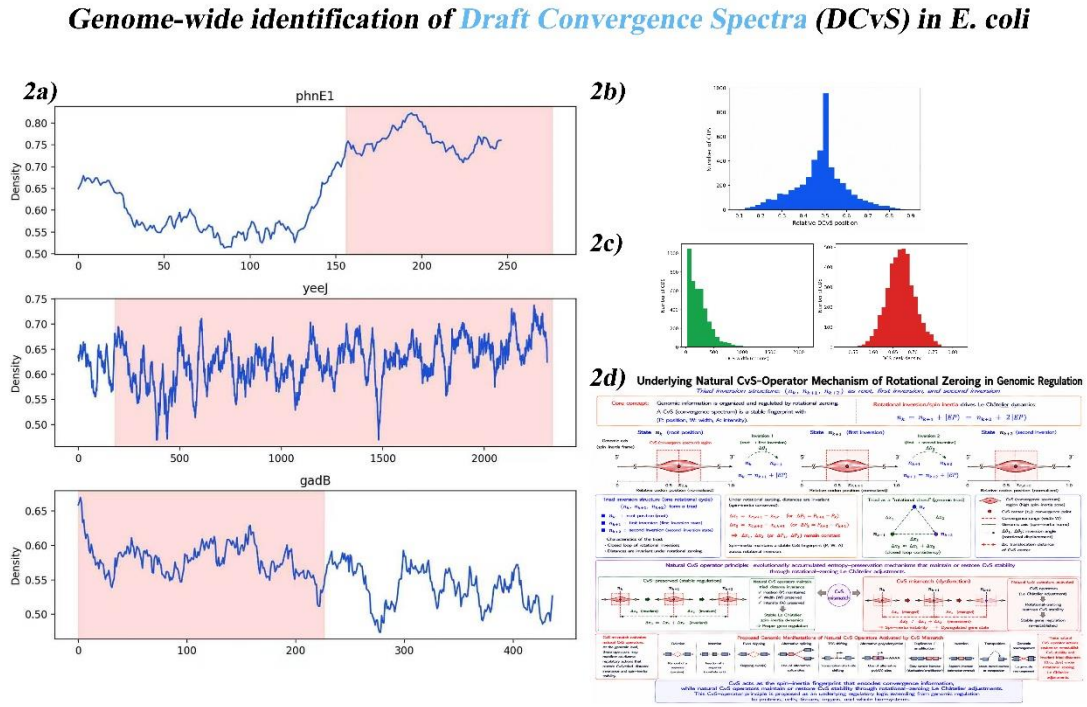
3.2.4 Genome-wide Identification and Characterization of Draft Convergence Spectra in *E. coli*

The identified Draft Convergence Spectrum (DCvS) regions were summarized across the analyzed *E. coli* CDS dataset. The extracted DCvS parameters, including relative position, width, and peak density intensity, were used for genome-wide characterization of the positional, spatial, and intensity organization of DCvS.

A total of **4,318 CDS sequences** were initially obtained from the reference genome. **Ninety CDS sequences** that did not satisfy the 30-codon minimum sliding-window requirement were excluded from density-landscape analysis, leaving **4,228 CDS sequences** for genome-wide DCvS identification (**S_Dataset 3**).

Representative rare-codon density landscapes and their corresponding DCvS regions are illustrated for three selected CDSs, ***phnE1, yeeJ,*** **and** ***gadB***, in **Fig. 2a**. The genome-wide distribution of relative DCvS positions is shown in **Fig. 2b**, while the distributions of DCvS width and peak density intensity are shown in **Fig. 2c**. Together, these parameters characterize the positional, spatial, and intensity organization of the identified DCvS regions. **These genome-wide DCvS characteristics further provide the empirical basis for examining the underlying natural CvS-operator mechanism of rotational zeroing illustrated in Fig. 2d.**

Figure 2. Genome-wide identification and characterization of Draft Convergence Spectra (DCvS) in *E. coli* (GCF_000005845.2) coding sequences (S_Dataset 1). (a) Rare-codon density landscapes of three representative CDSs (***phnE1, yeeJ,* and *gadB***), with shaded regions indicating the identified DCvS regions (**S_Dataset 2**). **(b)** Genome-wide distribution of relative DCvS positions across the 4,228 analyzed CDSs (**S_Dataset 4**). **(c)** Genome-wide distributions of DCvS widths and peak density intensities (**S_Dataset 5**). **(d) Underlying natural CvS-operator mechanism of rotational zeroing in genomic regulation**, illustrated using the simplest triad structure (n_k, n_{k+1}, n_{k+2}), corresponding to the root, first-inversion, and second-inversion states. The model proposes that **CvS mismatch and the resulting loss of triad-distance invariance activate corresponding CvS operators to restore rotational-zeroing stability**. At the genomic level, routine regulatory actions—including deletion, insertion, exon skipping, alternative splicing, transcription-start-site shifting, alternative polyadenylation, duplication/amplification, inversion, transposition, and genomic rearrangement—are proposed as potential manifestations of such **genomic CvS operators**. These operators act through **rotational-zeroing Le Châtelier adjustments** to restore CvS and spin-inertia stability.



3 Conclusion

A discrete **Convergence Spectrum (CvS)** represents an intrinsic fingerprint of asymmetric physical rotational zeroing spin inertia across different levels of bio-systems. A vertebral column can be understood as a macroscopic manifestation of the natural inversion superposition of diverse Convergence Spectra from genomic, protein, tissue, organ, and somatic levels. The present preliminary *E. coli* rare-codon CvS analysis provides a concrete discrete framework for future construction of spinal vector maps. Although introduced here through the musical operators sharp (♯), flat (♭), and natural (♮), the **CvS operator principle** may extend across genomic, protein, cellular, tissue, organ, and somatic levels, with **CvS operators** representing natural entropy preservation regulations accumulated through evolution.

Beyond evolutionary significance, **CvS mismatch or dysfunction** may activate corresponding CvS operators to restore rotational-zeroing stability, providing a potential underlying physical logic for genomic regulation and, more broadly, for regulation across protein, cellular, tissue, and organismal levels. **Persistent failure or misregulation of CvS operators may result in pathological CvS dysfunction across genomic, cellular, and tissue levels, potentially contributing to tumor**

metastasis. This concept suggests a potential system-level rotational-zeroing approach for future cancer research.

Interestingly, the genomic CvS identified from *E. coli* rare-codon organization exhibits a non-central positional bias, located predominantly within the **40–60% region** of CDS sequences. This CvS distribution shows positional correspondence with the **E–F CvS region of the C-major scale**, further suggesting a possible asymmetric entropy rotational-zeroing pattern. Whether this CvS (operator) position pattern can be extended to other species or across biological kingdoms remains an subject for further study.

Competing interests

The authors declare that they have no known competing financial interests or personal relationships that could have appeared to influence the work reported in this paper.

Authors' contributions

Y.L. perceived the models, performed the experiments with data collection help, and wrote the manuscript.

Supplementary Materials entitled **"*Spin Inertia Convergence Spectrum*"** include the following**: I. Supplementary Historical Documents**, providing supporting materials for the physical training and zeroing practices described in (Fig. 1b); **II. Supplementary Movie**, providing dynamic MRI observations associated with CSF rotational zeroing; and **III. Supplementary Datasets**, providing the numerical and source data underlying the genome-wide identification and characterization of **Draft Convergence Spectra** (**DCvS**) in *E. coli*. are available at the designated repository: https://www.scidb.cn/en/anonymous/Wlp6bUFm

with Data CSTR: https://cstr.cn/31253.11.sciencedb.010pk and

Data DOI: https://doi.org/10.57760/sciencedb.010pk

References

[1] Lai, Y. Quantum Gravity Non-simultaneous EP Irrotational Entropy Preservation Origin of Life. *IJSR*, **15 (1)**, 440-460 (2026). https://dx.doi.org/10.21275/ SR251231101432,
DOI: 10.21275/ SR251231101432

[2] Needham, J. (1959). Science and Civilisation in China, Vol. 3: Mathematics and the Sciences of the Heavens and the Earth. Cambridge University Press, p. 21.

[3] Clausius, R. Ueber verschiedene für die Anwendung bequeme Formen der Hauptgleichungen der mechanischen Wärmetheorie. *Annalen der Physik und Chemie*, **125**, 353-400 (1865).

[4] Boltzmann, L. Über die Beziehung zwischen dem zweiten Hauptsatze der mechanischen Wärmetheorie und der Wahrscheinlichkeitsrechnung, respective den Sätzen über das Wärmegleichgewicht. Sitzungsberichte der kaiserlichen Akademie der Wissenschaften Wien, *Mathematisch-Naturwissenschaftliche Classe*, Band 76, Abt. II, pp. 373-435 (1877).

[5] Shannon, C. E. A Mathematical Theory of Communication. *Bell System Technical Journal*, **27,** 379-423, 623-656 (1948).

[6] Cardoso, J. G.. Geometry of curved space–times equipped with torsionful affinities and Einstein–Cartan's theory in two-component spinor form. *Canadian Journal of Physics*, **103(11),** 1119-1127(2025). https://doi.org/10.1139/cjp-2025-0134

[7] Berghofer, Philipp, Jordan François, Simon Friederich, Henrique Gomes, Guy Hetzroni, Axel Maas, and René Sondenheimer. Gauge Symmetries, Symmetry Breaking, and Gauge-Invariant Approaches. Cambridge Elements. Elements in the Foundations of Contemporary Physics. Cambridge: Cambridge University Press, 2023.

[8] Noether, E. Invariante Variationsprobleme. Nachrichten von der Gesellschaft der Wissenschaften zu Göttingen, *Mathematisch-Physikalische Klasse*, pp. 235-257(1918).

[9] Pearce, Ben K. D., Andrew S. Tupper, Ralph E. Pudritz, and Paul G. Higgs. Constraining the Time Interval for the Origin of Life on Earth. *Astrobiology* **18(3),**343–64 (2018):. https://doi.org/10.1089/ast.2017.1674.

[10] Lai, Y. Measuring the "Weight" of Human *in vivo* Bio-Inertia by Legendary Galileo Falling Body Experiments on a Commercial 10m Diving Platform and Gravitationally Inversion of Newton's Three Laws of

Motion into the Basic Laws of Evolution. *IJSR*, **10(9)**, 1301-1328 (2021).
https://dx.doi.org/10.21275/SR21829103822 DOI: 10.21275/SR21829103822

[11] Xing, J., Liu, X., Chen, X., Li, C., Zhang, H., Lai, Y. (2026). UV Intermittent Sterilization for Controlling *Aspergillus SPP* Dissemination and Preventing Aflatoxin Dairy Contamination: The Quantum Gravity Linearity Shifting Collapse Mechanisms Underline Bio-Systems and the Definition of Entropy-Stabilized Barycenter (EB). *Eng OA, 4*(5), 01-13.

[12] Quincke, H. Die Lumbalpunction des Hydrocephalus. *Berl. Klin. Wschr*. **28**, 929-933, 965-968 (1891).

[13] Needham, Joseph. Science and Civilisation in China, Volume 4: Physics and Physical Technology, Part 1: Physics. Cambridge: Cambridge University Press, 1962. (especially discussions on Chu Tsai-Yü and the equal temperament system.)

[14] Pasterski. S. Asymptotic Symmetries and Electromagnetic Memory. *JHEP* **09**, (2017) 154

[15] Jinek M, Chylinski K, Fonfara I, et al. A programmable dual-RNA–guided DNA endonuclease in adaptive bacterial immunity. *Science*. 2012;337(6096):816-821

[16] Wing, C. E. & Chook, Y. M. Multiple roads between the nucleus and the cytoplasm: classes of linear NLSs and NESs and their receptors. *Curr. Opin. Struct. Biol.* **98**, 103244 (2026).

[17] Miller, S. L. Production of Amino Acids Under Possible Primitive Earth Conditions . *Science*. **1953**, 117: 528. doi:10.1126/science.117.3046.528

[18] Gilbert, W. Origin of life: The RNA world. *Nature* **319**, 618 (1986).

[19] Chai, P. et al. GlycoRNA complexed with heparan sulfate regulates VEGF-A signalling. *Nature*, **651,** 808-817(2026)